Review

A Review of CCUS in the Context of Foams, Regulatory Frameworks and Monitoring

Alirza Orujov [1], Kipp Coddington [2] and Saman A. Aryana [1,*]

1. Department of Chemical & Biomedical Engineering, University of Wyoming, Laramie, WY 82071, USA
2. School of Energy Resources, University of Wyoming, Laramie, WY 82071, USA
* Correspondence: saryana@uwyo.edu

Abstract: Greenhouse gas emission into the atmosphere is considered the main reason for the rise in Earth's mean surface temperature. According to the Paris Agreement, to prevent the rise of the global average surface temperature beyond two degrees Celsius, global CO_2 emissions must be cut substantially. While a transition to a net-zero emission scenario is envisioned by mid-century, carbon capture, utilization, and storage (CCUS) will play a crucial role in mitigating ongoing greenhouse gas emissions. Injection of CO_2 into geological formations is a major pathway to enable large-scale storage. Despite significant recent technological advancements, mass deployment of these technologies still faces several technical and non-technical difficulties. This paper provides an overview of technical milestones reached thus far in CO_2 capture, utilization, geological storage, monitoring technologies, and non-technical aspects such as regulatory frameworks and related policies in the US and the rest of the world. This paper describes different injection methods to store CO_2 in various subsurface formations, the use of foams and the resulting potential gains in CO_2 storage capacity, the role of nanoparticles for foam stabilization, and ensuring long-term storage safety. This work also addresses several safety-related aspects of geological storage and subsurface monitoring technologies that may mitigate risks associated with long-term storage.

Keywords: carbon utilization; nanoparticle-stabilized foams; geologic storage; policy; monitoring

1. Introduction

Global climate change is evidenced by disruptions in historical geographical and seasonal climate patterns. Persistent increases in the globally averaged surface air temperature are prominent features of these changes. The average temperature of Earth's surface has increased by approximately one degree Celsius (1.8 degrees Fahrenheit) since the late 19th century [1]. These changes have accelerated rates of the mean sea level rise [2]. Human activities and the associated greenhouse gas (GHG) emissions, especially those emitted since the industrial revolution, are the main culprits of the ongoing changes in the Earth's climate [3]. GHGs trap atmospheric heat [4] by absorbing infrared radiation from the sun [5]. These gases comprise a range of substances whose atmospheric concentrations considerably affect the global mean temperature [6]. According to the Fifth Intergovernmental Panel on Climate Change (IPCC) Assessment Report, the most critical GHGs based on their relative concentration and global warming potential comprise carbon dioxide (CO_2), methane, nitrous oxide, chlorofluorocarbon-12 (CFC-12), hydrofluorocarbon-23 (HFC-23), sulfur hexafluoride, and nitrogen trifluoride [7]. CO_2 accounts for approximately 76–79% of annual global GHG emissions [4,6,8]. The monthly average Mauna Loa concentration of CO_2 for September of 2022 was reported as 415.95 ppm [9]. In 2020, CO_2 emissions comprised 79% of the total anthropogenic GHG emissions in the US, of which 92% were due to fossil fuel combustion [10]. Despite a reduction in global energy demand and CO_2 emissions by approximately 5.1% in 2020 due to the COVID-19 pandemic, the world experienced a fast economic recovery in 2021. A 5.9% increase in economic output in

2021 was associated with a 6% rise in CO_2 emissions, making 2021 the most significant year-over-year increase in energy-related CO_2 emissions [11]. Developing Asian countries, especially China and India, significantly contribute to increasing global CO_2 emissions [12]. CO_2 emissions must be substantially curtailed worldwide in all sectors of the economy to prevent further global temperature rises [13]. To this end, the Paris Agreement was negotiated in 2015 as a legally binding international treaty on climate change. This agreement was adopted by 196 Parties at the twenty-first session of the Conference of the Parties (COP) in December 2015 and entered into force on 4 November 2016 [14]. The main objective of the agreement is "[h]olding the increase in the global average temperature to well below 2 °C above pre-industrial levels and pursuing efforts to limit the temperature increase to 1.5 °C above pre-industrial levels . . . " (Paris Agreement, Art. 2(1)(a)) [15]. The implementation of the agreement requires significant economic and social transformations [15]. The energy sector is responsible for approximately three-quarters of GHG emissions. To achieve the Paris Agreement's main objective, global CO_2 emissions must be reduced to net zero by 2050 [16]. This reduction will necessitate a complete transformation of our means of energy production, transport, and consumption [17]. Climate-change-related problems and increasing scarcity of natural resources compel the world community to better manage energy demand and supply and transition to a sustainable energy system. Such a transformation requires a combination of energy efficiency, renewable energy use (solar, wind, biomass, hydroelectric, etc.), and carbon capture and storage [18].

Energy-related and industrial processes are responsible for approximately 80% of CO_2 emissions [19]. According to the International Energy Agency (IEA), in 2020, about 78% of the world's energy needs were met by fossil fuels (e.g., oil, natural gas, and coal) and the remaining 22% by nuclear, biofuel, hydro, and other sources [20]. These figures represent an increase of 3% in renewable energy use, with electricity generation from renewable sources having risen by 7% to account for approximately 29% of global electricity generation in 2020 [21]. A profound transformation from fossil-fuel-dependent to renewable-energy-based systems enhances energy efficiency. The International Renewable Energy Agency (IRENA) reports that renewables may account for up to two-thirds of the global primary energy supply by 2050 [22]. According to a report by the IEA, solar PV and wind make up two-thirds of the renewable energy growth. IRENA estimates that energy efficiency and renewable energy can, together, contribute 90% of the mitigation measures needed to reduce energy-related emissions. That means the energy-related CO_2 emissions must fall by approximately 3.8% every year until 2050 to achieve levels 70% below today's level and meet the goals of the Paris Agreement [19].

Countries around the globe are making a concerted effort to increase the use of renewable energy sources. China is a prominent example, as it became the largest CO_2 emitter in 2019, accounting for approximately 27% of global CO_2 emissions [23]. More than 86% of China's primary energy consumption was accounted for by coal, natural gas, and petroleum [24]. Despite these figures, China is also a leading country in terms of installed renewable energy capacity. According to the IRENA, China generated about 329,000 MW of electricity from renewables in 2021. Meanwhile, the United States (US) generated only about 133,000 MW, followed by Germany and India with 64,000 MW and 40,000 MW of generation, respectively [25]. In the US, about 20% of all electricity was generated by renewable energies in 2021. Among different renewable sources, wind and hydro power contributed the highest amount to power generation in 2021, while wind and solar are expected to contribute more than 60% of the utility-scale electricity generation capacity to the US power grid [26]. The European Union's European Green Deal aims to neutralize the EU's carbon emissions by 2050 [27]. One of the main challenges of renewable energy is the need to create a flexible energy supply similar to that of fossil fuels. Fossil-fuel-based global systems can meet energy demands at the right time and place due to their large-scale storage capabilities of energy-dense liquid, gas, or solids [28]. A shift towards a more sustainable energy system has proven more challenging in some sectors, such as the transportation sector, which still utilizes an increasing amount of fossil fuels [29]. The best-

case energy transformation scenario will produce approximately 9.5 Gt of energy-related CO_2 emissions in 2050. Energy transformation scenarios may reduce emissions by over 75%. The remaining 25% may be reduced through carbon capture, utilization, and storage (CCUS); material efficiency; and the circular economy [19].

This paper addresses various fundamental aspects of CCUS, emphasizing foams and the legal and regulatory frameworks necessary for at-scale geologic carbon sequestration. This paper proceeds with a description of capture, utilization, and storage, followed by an expanded review of various considerations with respect to injection methods; foams, long-term storage, security, policy and regulations, and monitoring (see Figure 1). A description of the conclusions completes the paper.
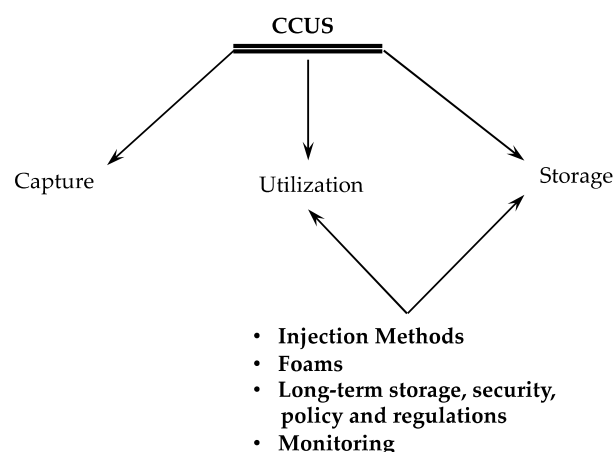

Figure 1. Scope of the paper.

2. CCUS

Significant amounts of CO_2 are produced and emitted into the atmosphere due to industrial processes [30]. CCUS is necessary to significantly reduce carbon dioxide emissions in the near term [31]. The CCUS supply chain comprises capture and compression of CO_2, as well as transportation of CO_2 to utilization and geologic storage sites [32]. It is predicted that carbon capture and storage will prevent about 32% of GHG emissions by 2050 [33].

The efficacy and adoption of utilization and sequestration of captured CO_2 depend heavily on the availability of technology elements and favorable economic drivers. Leonzio et al. [34] use a mathematical model to assess the optimal supply chain of CCUS in the UK. Considering the net present value and the payback period of different utilization and storage options, they concluded that the geologic storage of captured CO_2 is the most economical pathway [34].

The US Department of Energy (DOE) reports that the US has more than 2400 billion metric tons of CO_2 storage capacity in saline aquifers, unminable coal seams, and oil and gas reservoirs [35]. A 2021 report by the IEA indicates that CCUS facilities around the globe have approximately 40 Mt of capture capacity each year [36]. However, the applications of CCUS technologies are complex. They depend on several factors, such as a detailed understanding of geology, geoengineering, geophysics, environmental impact, and related mathematical and computer science know-how [37].

2.1. Carbon Capture

CO_2 separation and capture technologies for flue gas streams are commercially available [36]. Examples include direct air capture (DAC), precombustion, post combustion, and oxyfuel combustion [14].

2.1.1. Direct Air Capture

Unlike point-source capture from industrial sources, DAC refers to the capture of CO_2 directly from the atmosphere and includes two main technologies: liquid and solid DAC.

Liquid capture passes air through a solution, such as hydroxide, while solid DAC uses solid sorbent filters that chemically bind with carbon dioxide [38,39]. The world's first and largest climate-positive DAC and storage plant, Orca, launched in September 2021 in Hellisheidi, Iceland. Orca is located near the Hellisheiði geothermal power plant, runs entirely on renewable energy, and has around 4000 tons of CO_2 capture capacity yearly [40]. According to the IEA, there are 19 DAC plants currently operating worldwide, which capture more than 0.01 Mt of CO_2 per year. An additional 1 Mt of annual CO_2 capture capacity is in an advanced development stage in the US [38].

2.1.2. Precombustion Capture

The precombustion method refers to capturing and removing CO_2 before combustion is completed [41]. Precombustion CO_2 capture is usually associated with high CO_2 concentrations (15–60% by volume) and high-pressure and high-temperature process streams [42,43]. In precombustion, fossil fuels are converted to syngas (a mixture of CO and H_2). Syngas is typically produced by adding either steam (i.e., steam reforming) or oxygen (i.e., partial oxidation or gasification) to the primary fuel. In both cases, the process is followed by a water–gas shift reaction [44]. This water–gas shift reaction converts CO and water to CO_2 and H_2-rich gas. CO_2 can be separated, and H_2-rich fuel can be combusted [41].

2.1.3. Post-Combustion Capture

Post-combustion capture refers to removing CO_2 from the product flue gas stream. CO_2 may be removed from hydrogen-rich gases using a physical solvent [12]. The main adsorbents for the post-combustion process include activated carbon, metallic oxides, alumina, and zeolites. Regeneration of adsorbents requires heat (temperature swing adsorption) or a reduction in pressure (pressure swing adsorption) [45,46]. The leading post-combustion technologies rely on adsorption, physical and chemical absorption, cryogenics separation, and membranes [45,47]. Aqueous amine solutions (chemical absorption) are the most mature technology for removing CO_2 from natural gas. Recent improvements in polymeric membrane technology have enabled CO_2 capture from coal-fired power plants and related combustion sources [48].

Dissolution of CO_2 requires high pressures, with CO_2 released once more as the pressure drops. The precombustion approach does not require heat for solvent regeneration, and the removed CO_2 can be released above atmospheric pressure. Therefore, precombustion capture and compression of CO_2 may be twice as efficient as post combustion. Disadvantages of precombustion capture include a loss of the potential for power generation due to the removal of CO that may otherwise be burned in the turbine to generate power. Additionally, natural gas or syngas (conventional) turbines are more efficient than hydrogen-burning gas turbines [49].

2.1.4. Oxyfuel Combustion

Oxyfuel combustion technologies are among the leading technologies for CCUS. The main principle of oxyfuel combustion is the burning of the fuel using pure oxygen instead of air, which allows for improved control over flame temperature and recycling of a portion of the flue gas back to the furnace. The advantage of the oxyfuel method is that it generates a highly concentrated CO_2 flue stream, which eases the post-separation process [50], and it only requires CO_2 in most combustion systems [51]. The optimal oxygen concentration for the oxyfuel process is approximately 97% oxygen purity [52]. Oxyfuel combustion in power generation comprises four units: an air separation unit (oxygen production), a gas turbine or boiler (heat generation), a flue gas processing unit (quality control system), and a CO_2 processing unit (CO_2 purification, transport, and storage) [50].

The use of oxygen instead of air in oxyfuel combustion results in more efficient combustion [53]; it decreases fuel consumption and helps to obtain more than 80% volume

concentrated CO_2 stream, which makes purification easier through mechanical separation [51,54].

2.2. Utilization

CO_2 is often considered a waste product in the context of flue gases. Recent crises have led to the exploration of the use of CO_2 in various applications, which has turned CO_2 into a potentially valuable product [55]. Through carboxylation reactions, CO_2 can be employed to produce various chemicals [56]. Moreover, CO_2 can be directly applied for compound extraction, e.g., in enhanced oil recovery (EOR), the food industry, and dry cleaning [56]. CO_2 can also be incorporated into construction and building materials [55]. This paper classifies CO_2 utilization technologies into (i) CO_2 to products and (ii) geological categories [57].

2.2.1. CO_2 to Products

CO_2 may be used as raw material in products such as beverages and food, inorganic chemicals, fertilizers, fuels, agricultural goods, building materials, etc. [57]. Methanol, formic acid, urea, cyclic carbonates, and salicylic acid are the most common products that can be obtained via CO_2 [58]. The United States National Academy of Sciences (NAS) categorizes CO_2-based products into long-lived and shorter-lived products. Long-lived CO_2-based products are durable, with more than 100 years of carbon storage capacity. In contrast, shorter-lived products may be recycled as part of the circular carbon economy over a shorter time span [59].

CO_2 to Methanol

The idea of upgrading CO and CO_2 to produce methanol dates back to the 1970s [60]. Large-scale methanol production is possible through the following reactions [61,62]:

$$CO + 2H_2 \leftrightarrow CO_3O \tag{1}$$

$$CO_2 + H_2 \leftrightarrow CO + H_2O \tag{2}$$

$$CO_2 + 3H_2 \leftrightarrow CO_3OH + H_2O \tag{3}$$

The first reaction is methanol synthesis from CO, the second is a reverse water–gas reaction, and the third is methanol synthesis. Recently, Nobel Prize winner George A. Olah advocated for a term called "methanol economy", in which captured CO_2 from the atmosphere and H_2 produced from renewable energy sources can be used to produce methanol and used as fuel and raw material for synthetic hydrocarbons [63]. Although hydrogen is considered a clean energy source and plays an essential role in the chemical industry, it is not easy to store and transport, restricting its wide-scale adoption as an energy carrier. On the other hand, methanol is an excellent H_2 source with low toxicity. Low-chain alcohols are considered an alternative, more accessible pathway to transport and store hydrogen [64]. Methanol may be mixed with conventional gasoline without requiring technical modifications of vehicles [65]. Around 90% of methanol is produced from natural gas [66].

CO_2 to Formic Acid and Urea

Urea is an essential product that can be obtained from CO_2. Urea is the most widely used synthetic nitrogen fertilizer and accounts for about 70% of worldwide fertilizer usage [67]. Urea has a high nitrogen content (up to 46%) and is most commonly produced through the following reactions [58]:

$$N_2 + 3H_2 \rightarrow 2NH_3 \tag{4}$$

$$CO_2 + 2NH_3 \rightarrow NH_2CONH_2 + H_2O \tag{5}$$
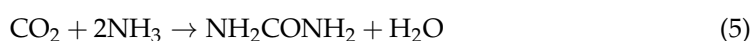
Urea production requires fossil fuels, which leads to greenhouse gas emissions. In urea production, natural gas is purified and converted to syngas in a reforming unit [68].

Agriculture and other land use contribute significantly to GHG emissions, according to the IPCC. These activities accounted for about 23% of anthropogenic CO_2 emissions between 2007 and 2016 [16]. However, the contribution of agricultural activities to the global carbon cycle is complex. Nitrogen-based synthetic fertilizers can change forest carbon distribution [69]. Results from a worldwide meta-analysis from 1998 to 2021 proved that nitrogen fertilizers significantly decrease soil bacterial and fungal diversity, affecting the soil's important carbon content [70]. Adding nitrogen to soil also plays a critical role in soil respiration. Soil respiration is also temperature-sensitive, and increasing average global temperature and increasing nitrogen-based fertilizer usage can significantly affect the cycle [71].

Formic acid is also an essential and often-used commodity in the chemical industry. It can be obtained in various ways, including the CO_2 hydrogenation reaction shown below to synthesize formic acid using CO_2 as raw material [72]. The worldwide production capacity of formic acid is approximately 950 thousand tons per year [73].

$$CO_2 + H_2 \rightarrow HCOOH \tag{6}$$

Life cycle assessment of several CO_2-based chemicals shows that CO_2-based production of formic acid reduces the environmental impact significantly [58,74]. Most of the produced formic acid is used in silage for animal feeds, as tanning and dyeing agents in the textile industry, as a coagulating agent for latex rubber production, and as a food preservative [75].

2.2.2. Biological Sequestration

Photosynthesis is the conversion of solar energy into chemical energy by green plants and certain other organisms. Carbohydrate molecules synthesized from water and CO_2 can store this chemical energy [76]. The overall oxygenic photosynthesis reaction can be expressed as [77]:

$$CO_2 + H_2O \rightarrow (CH_2 O) + H_2O + O_2 \tag{7}$$

A single mature tree can absorb about 50 pounds of carbon dioxide annually. This absorption rate means that approximately 200 billion trees are needed to remove the CO_2 emitted in the US annually [78]. However, some microorganisms and microalgae have higher carbon fixation rates than terrestrial plants [79]. Generally, there are two main biological processes for biological carbon sequestration: (i) biomass for energy generation with CO_2 capture and (ii) the photosynthetic systems of microorganisms [80]. Microalgae can transport bicarbonate into their cells with as high as 90% efficiency and harvest 100% of the biomass [81].

2.2.3. Geologic Utilization

Geological utilization of CO_2 mainly comprises applications for subsurface energy extraction, including enhanced oil recovery (CO_2-EOR), hydrocarbon production from residual oil zones (ROZs), coalbed methane, and CO_2-enhanced shale gas recovery [57].

CO_2-EOR

The most substantial use of CO_2 is in enhanced oil recovery [55]. During the life of a petroleum reservoir, the fluids are typically produced initially by a natural drive mechanism such as a gas cap or dissolved gas expansion and saline water influx. This production is possible until the reservoir pressure and oil production rates decline. At that point, a secondary recovery phase, referred to as improved oil recovery (IOR), begins, which is most commonly achieved by injecting water [82]. Under favorable conditions, primary recovery and IOR may produce up to one-third of the oil that was originally in place. The remaining oil, estimated to be more than 5000 billion barrels worldwide, may be accessed and produced using EOR techniques such as "next generation" CO_2-EOR [83]. Recovery techniques that are applied after a primary and a secondary recovery phase are referred to as tertiary recovery, and EOR often falls in that category, even though CO_2 EOR may

be applied during the secondary recovery phase, such as in the North Cross field in West Texas [82,84]. CO_2-EOR has been studied and applied in several experimental projects since the 1950s [85]. According to a recent report from the IEA, about 375 active EOR projects supplied about 2% of the global oil supply in 2017, of which 166 were CO_2-EOR projects [86].

Most reservoirs under CO_2-EOR projects are deep enough and are pressurized beyond the minimum miscibility pressure (MMP) of CO_2 [87]. For reference, the Yates field in West Texas is an example of an immiscible CO_2 flood [88]. Main CO_2 EOR mechanisms include oil viscosity reduction, the oil-swelling effect, interfacial tension reduction, light-hydrocarbon extraction, and miscible displacement if the reservoir pressure exceeds its MMP [85]. The density of supercritical CO_2 approaches that of a liquid, but its viscosity remains quite low [87]. CO_2 flooding approaches include CO_2 huff-n-puff, continuous CO_2 flooding, and CO_2 water-alternating-gas (CO_2-WAG) methods [89]. Supercritical CO_2 flooding has been demonstrated to improve the oil recovery factor in unconventional reservoirs [90].

Residual Oil Zones

A ROZ is defined as residual oil with respect to waterflood below the oil-water contact (OWC) of a reservoir. ROZs are similar to classical reservoirs after a mature waterflooding process, the difference being that ROZs have essentially been flooded by natural aquifers [91]. Although primary or secondary oil production from ROZs is often not economical, CO_2 flooding is a viable recovery technique [92]. Three primary types of ROZs are identified [93]: (i) One type of ROZ happens because of a regional tilt of a basin. This type occurs when an existing hydrocarbon reservoir (stratigraphic trap) is subjected to a tectonically induced tilt [94]. (ii) Another type of ROZ is due to water invasion of areas that are subject to migration of trapped oil through breached seals. (iii) The final type of ROZ is similar to type one, the difference being that they are a result of changes in hydrodynamic conditions of groundwater [93,94]. CO_2-EOR is an increasingly used technique for oil production from ROZs, especially in the Permian Basin [93,95,96]. ROZs are also considered potential targets for long-term geologic carbon storage [97]. CO_2 storage in ROZs is mainly impacted by reservoir heterogeneity and injection strategies [98]. For example, in the case of vertical CO_2 injectors, high ratios of WAG always result in higher retention fractions; however, this process results in a reduction in cumulative CO_2 injection. Therefore, different strategies may be applied depending on whether the intention is to maximize oil production or enhance storage [98]. Since EOR contributes to anthropogenic GHG emissions, whether CO_2-EOR will result in a net CO_2 reduction is an ongoing discussion. Comparisons indicate that one barrel of oil recovered by CO_2-EOR has a lower CO_2 emission than one barrel produced through primary recovery or IOR [55].

Enhanced Gas Recovery in Coalbed Methane

Coalbed methane (CBM) is considered an unconventional gas reservoir. Methane in coalbeds is stored on the internal surfaces of microporous coal as sorbed gas near liquid densities [99]. CBM is also called coal seam methane, coal seam gas, and coal seam natural gas and may contain trace amounts of other fluids [100]. CBM can be a significant hazard for coal mine development, with the potential for explosions ignited by different sources during mining operations and causing severe causalities [101]. Since the 1970s, CBM has been successfully developed into a commercially and economically sustainable product, primarily in the United States and Canada [102]. Conventional CBM recovery is based on the pressure depletion strategy of the reservoir. Removing water from the reservoir reduces the pressure, and some gas desorbs from the coal [99]. The main problems associated with CBM development are the low permeability of coal beds and high methane adsorption. Therefore, CBM development techniques involve injecting various materials, including water, CO_2, and steam [103]. Injecting supercritical CO_2 in the coal seam can enhance methane recovery considerably [104]. CO_2-enhanced coalbed methane (ECBM) is based

on competitive sorption between CO_2 and methane on coal. CO_2 has more significant adsorption than methane, resulting in the desorption of existing methane when injecting CO_2 into a coal bed [105].

2.3. Storage

The captured CO_2 must be permanently stored to mitigate the adverse effects on the global climate [106]. Long-term CO_2 storage may be possible through underground sequestration in sedimentary formations and carbon mineralization [107]. Between the two, CO_2 sequestration in the subsurface is a mature technique and may be applied to different sedimentary formations [106]. Geological formations can store massive amounts of CO_2. Examples include oil and gas reservoirs, deep saline aquifers, silicate formations, and unminable coal streams [55]. It is estimated that up to 11,000 Gt of CO_2 may be stored in subsurface formations. In contrast, the 2022 global energy-related CO_2 emissions reached 36.8 Gt [108].

Saline aquifers are brine-saturated layers of porous rock and are more extensive than oil-and-gas-bearing rocks or coal streams [109]. Saline aquifers are estimated to hold most of the overall geologic storage potential [110–112]. The estimations of this potential storage fall within a wide range due to differences in assumptions such as density, characteristics of aquifers, technological and economic constraints, and whether CO_2 remains as a separate fluid phase or dissolves in brine. The upper limit of the storage capacity of saline aquifers is uncertain due to insufficient geologic data [47]. Even though aquifers may be located near stationary CO_2 emission sites [113,114], their depth and high concentrations of dissolved salt contents make saline aquifers economically suboptimal. Hepple and Benson [115] concluded that 90–99% of injected CO_2 is expected to remain effectively trapped over thousands of years. Expertise related to transportation and injection aspects of geologic CO_2 storage is readily available in the EOR community [116]. Although there is no universally accepted definition of coal minability, some coal mines are accepted as qualitatively and economically unminable. The reasons may include the mines being too deep, having poor quality, and land use restrictions [117]. ECBM processes in unminable coal seams can permanently store CO_2. Although unamenable coal seams have a smaller CO_2 storage capacity than other geological formations, it is estimated that about 3 to 200 Gt of CO_2 can be stored globally in unminable coal seams [104].

Several industrial-scale CO_2 storage projects in saline aquifers are underway [112]. CO_2 injection in a saline aquifer has been operated in Canada to decrease H_2S flaring from sour gas wells [112]. The Sleipner project in the Norwegian part of the North Sea is considered the first commercial CO_2 storage project in deep aquifers. Injection in Sleipner started in October 1996, with 1 Mt of CO_2 injected yearly [118]. The In Salah project in Algeria is another example of CO_2 from the production of natural gas sequestered in the subsurface. This project is estimated to have saved the equivalent of 1.2 million tons of greenhouse emissions every year since 2004 [119]. A similar CO_2 injection project is implemented offshore in Norway in the Snøhvit field. The injection started in 2008, and the cumulative CO_2 injection is estimated to be equivalent to 2% of the total emissions of Norway over 30 years [120]. The Weyburn project in Canada is a large-scale CO_2-EOR storage project estimated to store 50 million tons of CO_2 over its lifetime [121]. CO_2 injection in saline aquifers is simpler than CO_2-EOR, since aquifers contain only brine. Furthermore, rates of injection into saline aquifers may be kept high while bottomhole pressures are kept relatively low. In general, there are three main CO_2 storage mechanisms, namely geochemical, geological, and hydrodynamic trapping [122] (see Figure 2). Amongst various trapping mechanisms, the following are considered the most significant in saline aquifers: structural, residual, solubility, and mineral trapping [114].
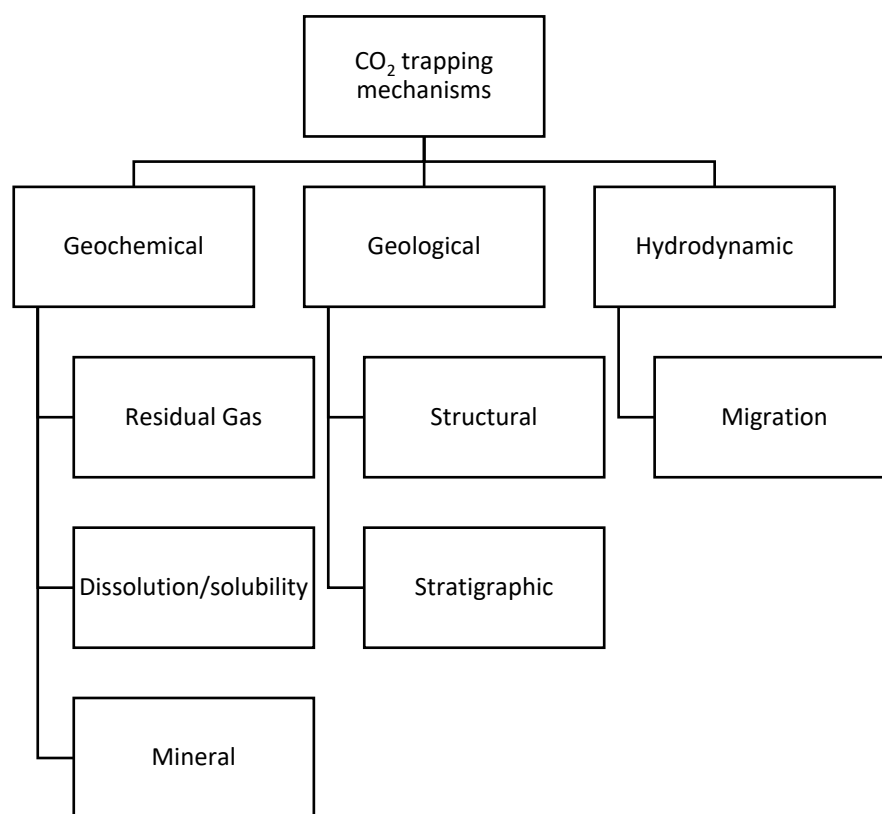
Figure 2. CO_2 trapping mechanisms.

Mineral trapping is a permanent storage mechanism in saline aquifers. Injecting a slug of brine after the completion of CO_2 injection may accelerate CO_2 dissolution [123]. Dissolved CO_2 reacts with the minerals in host formations and creates stable minerals over geological timeframes [124,125]. Solubility also plays a vital role in geological storage, depending on temperature, pressure, and salt content [126,127].

Since the goal is permanent geologic storage of CO_2, safety and storage reliability over the long term are paramount. As such, one must assess potential risks associated with the formation and activation of fractures [55]. Hazards include possible leakage of stored fluids through the caprock, degraded well cement, and transmissive faults and fractures [128]. Minimization of CO_2 mobility by mineralizing it into some form of the carbonate, such as limestone or magnesite, will reduce the amount of free and mobile CO_2. However, mineralization may occur on the order of the geological timescale. Research into improving and accelerating the mineralization process is ongoing in the community [129].

3. CO_2 Injection Methods

CO_2 flooding processes can be classified into miscible and immiscible, although CO_2 is not immediately miscible upon first contact with oil in the reservoir. CO_2 is, in general, soluble in crude oil at reservoir pressures above its minimum miscibility pressure (MMP—defined as the lowest pressure at which dynamic miscibility develops between oil and the solvent, i.e., injected CO_2 [87,130]) but the process is achieved after multiple contact miscibility processes [131]. Miscible CO_2 flooding effectively increases production rates and recovery and extends the economic life of assets [84]. As such, one must always consider the average reservoir pressure before CO_2 flooding versus MMP [132]. Miscibility depends on reservoir pressure, depth, and API gravity [133]. In such cases, immiscible CO_2 flooding may be a viable alternative [134]. Adel et al. [135] conducted several experimental gravity-stable CO_2 floods below and above MMP to determine the oil recovery factor. Although all miscibility conditions produced good recovery factors due to the gravity-stable floods, those above MMP resulted in a better recovery factor (98%) than those below MMP (89%).

Due to the lower density and viscosity of CO_2 than oil or water, CO_2 rises to the top of the reservoir, resulting in fingering and poor volumetric sweep efficiency [135,136]. Figure 3 provides a summary of CO_2 flooding methods.
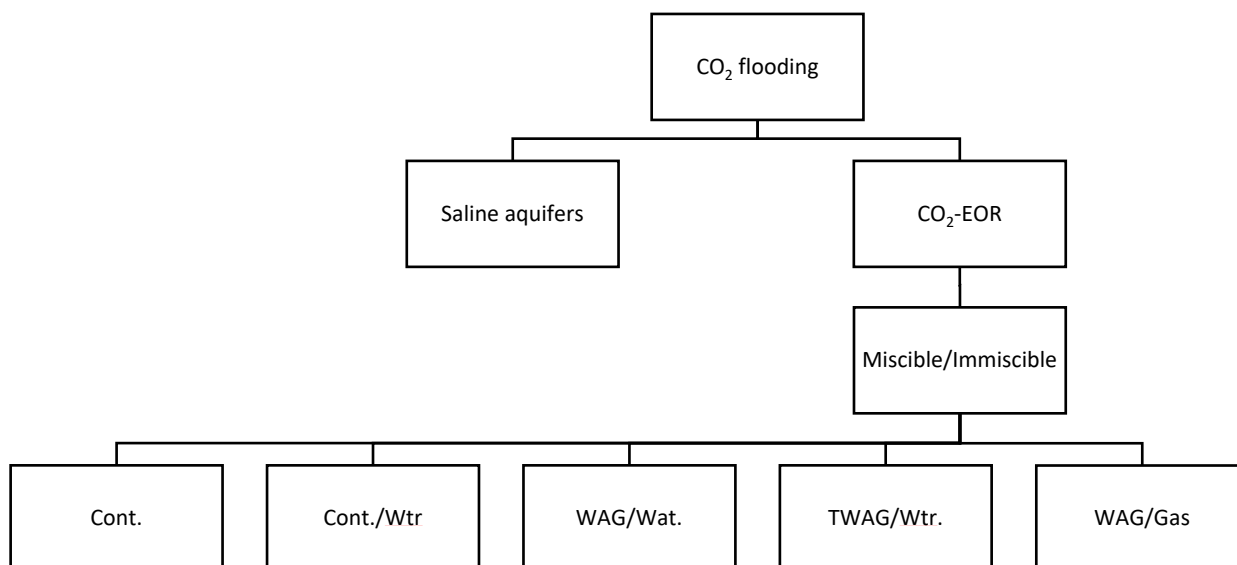

Figure 3. CO_2 flooding techniques: continuous CO_2 injection (Cont.), continuous CO_2 chased with water (Cont./Wtr.), conventional alternating CO_2 and water chased with water (WAG/Wat.), tapped alternating CO_2 and water (TWAG/Wtr.), and alternating CO_2 and water chased with gas (WAG/Gas).

3.1. Continuous CO_2 Flooding

During continuous CO_2 floods, a CO_2 slug is continuously injected into the formation [87]. Compared to other CO_2 flood schemes, continuous CO_2 injection requires a more straightforward system, which helps the project's economics at the early injection stage. Nevertheless, after breakthrough, the produced gas–oil ratio (GOR) rapidly increases, necessitating high CO_2 separation and recycling capacity [137]. Continuous CO_2 floods are often limited to two reservoir types: (i) reservoirs that are suitable for gravity-stable displacements and (ii) those that are not suitable for water flood and may perform unfavorably in response to water injection [138]. Although continuous CO_2 injection may require more cumulative CO_2 volumes, it may perform better over the long term than other CO_2 floods in terms of throughput and incremental oil production [139]. In some cases, such as vertical downward CO_2 displacement projects, a lighter gas may follow CO_2 to maximize gravity segregation and minimize gravity through channeling [87].

3.2. Continuous CO_2 Chased with Water

Continuous CO_2 chased with water is a CO_2 flood that includes injection of chase water to help drive the CO_2 slug. This method is usually applied for low-heterogeneity reservoirs [140]. Such reservoirs often require minimal gas recycling and retain much of the injected CO_2. Chase water immiscibly displaces the mobile miscible CO_2 slug [87]. Luis et al. [141] simulated several years of continuous CO_2 injection followed by chase water injection. The results show an optimal CO_2 slug size for maximizing incremental oil production, and additional injection of CO_2 does not improve oil recovery much further [141].

3.3. Conventional WAG and Alternating CO_2 and Chase Water

Water-alternating gas (WAG) was proposed for EOR in 1966 [142]. The method aims to improve the sweep efficiency of injected gas by utilizing slugs of water for mobility control and front stabilization. WAG has a combined effect on increasing the displacement

efficiency, whereby the injected gas improves pore-scale displacement efficiency and the injected water improves the macroscopic displacement efficiency [143]. In CO_2 WAG, the injected CO_2 reduces oil viscosity and mobilizes otherwise immobile oil [144]. Improvements in recovery are especially notable for CO_2 when miscibility conditions are satisfied. As a result, light oil reservoirs are often preferred because miscibility is achieved at lower pressures [89]. During conventional WAG processes, a chase water slug is injected after the final slug of CO_2 is injected [87].

The injected gas and water volumes are essential for optimal displacement efficiencies during WAG. Injecting excess amounts of water may result in lower displacement efficiencies at the pore scale, and excess gas injection may result in poor vertical and horizontal sweep efficiencies [145]. For example, a study of Iranian reservoirs shows that the optimal WAG ratio is about one [146]. Chemical-alternating gas injection, called chemically enhanced water alternating gas (CEWAG), is a modification of the WAG scheme to improve performance. Other such examples include surfactant-alternating gas (SAG), polymer-alternating gas (PAG), and injection of low-salinity alternating gas (LSWAG) [147]. Foam-assisted water-alternating gas (FAWAG) is another WAG-inspired EOR technique. FAWAG may be considered an immiscible WAG injection method and may improve sweep efficiency, reduce the GOR, and maximize recovery [148,149]. Modifying injected water characteristics, such as its salinity, may also improve recovery by altering wettability and suppressing crude oil snap-off and microdissection formation [150].

3.4. Tapered Water-Alternating Gas (TWAG)

In tapered water-alternating gas (TWAG), predefined CO_2 slugs are injected intermittently and sandwiched between increasing water cycles until the total amount of CO_2 is injected. This method aims to decrease CO_2 utilization for each incremental barrel of oil [87]. Simulations of conventional WAG and TWAG using uniform WAG ratios in homogeneous and heterogeneous domains show that a 4-year water injection followed by a 1-year CO_2 injection (4:1) TWAG ratio yields the highest oil recovery [151]. Simulated miscible WAG and TWAG processes show that tapered WAG is more attractive for both homogenous and heterogeneous media [152].

3.5. Alternating CO_2 and Water Chased with Water (WAG/Gas)

Alternating CO_2 and water chased with water is similar to conventional WAG, except that once the designed CO_2 slug is injected, the CO_2 cycle is substituted with a less expensive gas cycle. The advantage of using chase gas is its potential to limit the CO_2 slug while maintaining miscibility [87].

4. Foams

CO_2 has a considerably lower viscosity than water and most crude oils. These differences in viscosity often lead to flow instability and adverse mobility ratios during CO_2 injection [136,153]. The resulting dynamics may cause viscous fingering and early gas breakthroughs. Additionally, the adverse density ratio of CO_2 to resident fluids often leads to gravity segregation and migration of CO_2 towards the formation's upper part, resulting in lower sweep efficiencies and inefficient gas storage and utilization [154]. To overcome the undesirable flow dynamics induced by adverse viscosity and density ratios, one may elect to decrease the mobility of the injected fluids, such as by using foams [155,156]. Application of foam for fluid mobility control has been investigated for several decades [157]. The main principle of foam flooding is to increase sweep efficiency by decreasing the mobility of the gas phase [158]. CO_2 foams may be injected using surfactant solutions, a water-alternating gas (WAG), or a co-injection scheme [159]. From a foam-generation perspective, foam flooding approaches include (i) direct foam injection using a foam generator and (ii) co-injection of gas and a surfactant solution using a WAG scheme [160]. The resulting foam has a much higher apparent viscosity than its constituents, increasing flow resistance in highly permeable zones and improving sweep efficiency [154,161,162]. Therefore, the

application of foams is especially beneficial in heterogeneous reservoirs [163]. For modeling purposes, simulation parameters may be estimated based on steady-state laboratory foam experiments of the effects of foam quality on its apparent viscosity [164]. Apparent foam viscosity is defined as

$$\mu_{foam,app} = \frac{-k\nabla p}{u_w + u_g},$$ (8)

where k is permeability, ∇p is the pressure gradient, and u_w and u_g represent the flux of the surfactant solution and the gas, respectively [164]. Foams are the dispersion of a large amount of gas inside a relatively small liquid volume. Thin liquid films separate the gas phase of the foam. Foams may be classified as wet or dry. Wet foams are composed of spherical bubbles separated by relatively thick liquid layers. In dry foams, thin film layers separate the bubbles. Foams with hydrocarbon-based fluids are referred to as nonaqueous foams. Foams are usually generated by agitating a mixture of liquid and a foaming agent, such as a mixture of a surfactant solution and gas [159,165].

4.1. Foam Characterization

Foams are characterized based on their quality and bubble sizes. Foam quality refers to the gas fraction in the foam, and bubble size is the average bubble diameter and distribution [159,165]. The quality of the foam is defined as the ratio of the gas volume to the total foam volume (gas + liquid) for a given temperature and pressure. Foam quality (FQ) is expressed as [166]

$$FQ = \frac{V_{gas}}{V_{gas} + V_{liq}},$$ (9)

where V_{gas} and V_{liq} refer to gas and liquid volume, respectively. FQ may be as high as 95%. Average bubble size and distribution may vary widely from colloidal size up to millimeters [165,167]. If the bubble size becomes larger, the foam is often less stable. Foaming agents (surfactant) also play an essential role. Surfactants are selected based on their foaming ability and the mobility and stability of the resulting foam [159]. The most commonly used surfactants are chemical and industrial surfactants, which are usually expensive and not environmentally friendly. Natural surfactants, such as Cedr extract (Zizyphus Spina Christi), often have a smaller footprint [168]. A low FQ results in a relatively low bubble count and apparent foam viscosity. At high FQ values, foams exhibit relatively high viscosities [166]. Foam quality can be modulated by adjusting the flow rate of the surfactant solution [169]. Results show that changing the flow rate of the surfactant solution while keeping a fixed gas injection pressure produces different foam qualities. Foam flow regimes in porous media are, at times, delineated into a high-quality and a low-quality regime: the high-quality regime refers to scenarios with high gas fractional flows (dry foam), and the low-quality regime refers to cases with low gas fractional flows (wet foam). The high-quality regime corresponds with longer foam propagation distances in low-permeability regions and flow diversion into low-permeability regions compared with the low-quality regime [169]. Examining FQ in in situ foam generation in fractured porous media with constant total superficial velocity and varying gas fractional flows indicates that oscillations in the pressure gradient in varying gas fractional flows decrease the time-averaged apparent foam viscosity [170]. CO_2 foam may also be generated by replacing a portion of CO_2 with nitrogen to optimize foam quality and oil recovery during EOR. Examining various gas ratios and FQs in supercritical CO_2/N_2 foams reveals their improved stability and viscosity compared with CO_2 foams [171].

Nevertheless, higher FQs do not always translate to higher oil recoveries due to a potential loss of foam stability [171]. The results of a series of steady-state CO_2 foam flow experiments at reservoir temperature and pressure conditions and different flow rates and foam qualities suggest that foam mobility may decrease with increases in FQ [172,173]. These results also show that foam mobility increases with increasing flow rates [172,174]. Increasing FQ has a direct nonlinear effect on foam strength until a maximum is reached,

after which a linear strength decline is observed [175]. The results show an optimum response at about 85% FQ, while an FQ of 95% quickly dried out, resulting in low foam strength. High foam strength indicates the effectiveness and robustness of the given surfactant in maintaining high dynamic surface tensions [175]. Apparent foam viscosity has a relationship with the injected gas fraction, and FQ [164]. The foam's apparent viscosity has a high-quality and low-quality regime. The apparent foam viscosity increases with increasing injected gas fraction in the low-quality regime. In contrast, in the high-quality regime, it decreases as the injected gas fraction increases. In the low-quality regime, the apparent foam viscosity increases with an increase in the injected gas fraction. In the high-quality regime, the apparent foam viscosity decreases with an increase in the injected gas fraction. The maximum apparent viscosity is observed at the boundary of two regimes known as transition foam quality [164].

Maximum apparent viscosity is obtained at the boundary of the two regimes at a given surfactant concentration and total superficial velocity. A transition in FQ is observed at the border of the two regimes for a given gas fractional flow [164]. The higher (compared with its constituents) apparent foam viscosity results in improved microscopic displacement and volumetric sweep efficiency and increased storage capacity [176]. Experiments show that apparent foam viscosity, which is a function of surfactant type, decreases as more CO_2 is injected [176]. Results from a capillary viscosimeter constructed for measuring the rheological properties of foams show that foams are pseudoplastic in nature, which is why they have several orders of magnitude higher apparent viscosity than their gas or liquid fractions [173]. It is essential to note the significance of the relationship between shear stress and shear rate in understanding rheology [173].

4.2. Foam Stability

Foams are thermodynamically unstable and will eventually collapse. The term stable in "stable foams" refers to a relative measure of stability in a kinetic sense. Several factors, including interfacial and bulk solution properties, determine stability. Foam stability may be assessed by measuring its half-life or average lifetime [159,177]. Foam stability in porous media is often described as the combined effect of drainage, coalescence, and coarsening. Coalescence is the merging of two or more bubbles and their impending collapse. Coarsening is the diffusion of gas from one bubble to another due to capillary pressure differences between neighboring bubbles [178]. Drainage is thinning of the liquid film due to gravity or capillary suction.

The bulk foam test is an essential experimental method to determine foam stability and formability. This test examines foam decay as a function of time (formability of foam) [179]. Foam injection is a dynamic process; foam is generated and coalesced during the injection. Drainage and coalescence drive the decrease in the height of the foam in an open system. Due to comparatively low diffusion rates, coarsening is insignificant during bulk foam tests [178,180,181]. Half-life is another critical parameter that indicates absolute foam stability. Half-life is the time it takes for foam height to decrease by half of its initial height.

A quantitative measurement known as dynamic foam equilibrium reveals the balance between foam generation and collapse, which is not usually investigated during bulk foam tests. The authors of ref. [154] investigated dynamic foam equilibrium, formability, and stability in foams stabilized using nanoclays and amorphous fumed silica and different surfactants [154]. Fan et al. [182] used molecular dynamics simulations to investigate surfactant concentration, temperature, and pressure influences on CO_2 foam interfacial tension (IFT) and stability. Results show that increasing the surfactant concentration decreases IFT and increases foam stability, while increasing the temperature causes a reduction in foam stability, with pressure having the opposite effect.

4.3. Nanoparticle-Stabilized Foams

Surfactant-stabilized CO_2 foams may experience instability caused by surfactant retention in porous media and high-temperature reservoir conditions, which limits their

applications in EOR [183,184]. One potential solution is the use of nanoparticles to further strengthen and stabilize foams for subsurface applications [154,162,184–188]. Rognmo et al. [189] experimentally proved that using silica nanoparticles to stabilize foam improves its stability and enhances the associated storage capacity. Higher nanoparticle adhesion energy to fluid interfaces than surfactants results in longer-lasting foams. Nanoparticle-stabilized foams may be stable over a year, whereas surfactant-stabilized foams often have a lifetime on the order of a few hours [184,190]. Experiments indicate that fly ash and recyclable iron oxide nanoparticles with LAPB-AOS surfactant mixtures are effective in stabilizing CO_2 foams, with fly ash-stabilized foams being the more stable of the two [183,191]. Results also show an incremental oil recovery of up to 90% of the oil that remains after a waterflood due to NP-stabilized CO_2 foams [183]. Foams that are stabilized with appropriately designed surface-modified nanoparticles show improved foam viscosity and stability compared with surfactant-stabilized foams under elevated temperature and pressure conditions for EOR and geologic CO_2 storage applications [192].

An essential advantage of nanoparticles for CO_2 foam stabilization is their ability to irreversibly absorb at CO_2–water interfaces and provide potential longer-term stability than traditional dynamically adsorbed and desorbed surfactants [193].

Contact angle is a key parameter to explain particle behavior at interfaces. IFT values between these phases regulate the contact angle between the surface of nanoparticles with CO_2 and water. As indicated by Young's equation (Equation (10)), the addition of surfactants causes a decrease in $\cos(\theta)$ by reducing the numerator ($\gamma_{SC} - \gamma_{SW}$) at a higher rate than the drop it causes in the denominator (γ_{CW}) [193]:

$$\cos \theta = \frac{\gamma_{SC} - \gamma_{SW}}{\gamma_{CW}}, \tag{10}$$

where γ_{cw}, γ_{sc}, γ_{sw} represent CO_2/water, solid/CO_2, and solid/water interfacial tensions, respectively. This decrease explains the reduction in hydrophilicity due to the adsorbed surfactant. Other important mechanisms include lamella drainage, disjointing pressure interfacial viscosity, and hole formation [193]. Even though direct inhalation of dry silica has deleterious defects on human health, silica nanoparticles are considered environmentally friendly and economically feasible for subsurface applications [194]. Surface-modified nanoparticles enhance foam stability considerably [195]. For example, experiments show the effectiveness of modified $Fe_3O_4@SiO_2$-700 (700 µL coated with tetraethyl orthosilicate) particles with a 68.5° contact angle in achieving a stable foam system [196] with the possibility to recycle and reuse the nanoparticles. Polyelectrolyte complex nanoparticles are also capable of developing highly stabilized lamella and environmentally friendly supercritical CO_2 foams [197]. They may offer a path to decrease freshwater usage, create more resilient lamella against surface tension variations at interfaces, and improve sweep efficiency.

4.4. Foam Formation Mechanisms

Foam formation may be accomplished by physical, chemical, or biological methods during the foaming process. Physical mechanisms involve mechanical foaming and phase transition. Chemical mechanisms involve chemical or electrochemical reactions, and biological mechanisms involve fungus-induced reactions. Foaming in porous media is accomplished by physical mechanisms [198]. There are three basic pore-level foam formation mechanisms: gas bubble snap-off, lamella division, and leave-behind.

4.4.1. Snap-Off

The snap-off mechanism occurs when gas invades pore throats, followed by liquid accumulation, eventually blocking the throat. Initially, a liquid lens forms but later drains from the lamella with a rise in the capillary pressure at the throat [199]. As the bubble penetrates the constriction and joins the stream, its expansion causes a decrease in the capillary pressure gradient. Consequently, a pressure gradient in the liquid phase allows flow from the surrounding liquid toward the neck of the constriction. This incoming liquid

surrounds the extended gas bubble and promotes its snap-off once capillary pressure drops below a critical level, which creates a separate gas bubble. Snap-off is the predominant foam-generation mechanism [159,200].

Gauteplass et al. [201] investigated pore-level foam generation, propagation, and sweep efficiency using a microfluidic model to accurately represent a sandstone sample in terms of grain size, shape, and pore structure. Snap-off is observed both in the interior of the porous network and at permeability discontinuities between the medium and the fracture [201]. Examination of bubble behavior in single and cascaded pore throats in micromodels shows that bubbles penetrate and pass through the throat, creating asymmetric dumbbell-like shapes. Due to the capillary effect, snap-off of the thin neck occurs in the throat. Smaller bubbles downstream are called daughter bubbles. The size distribution of these daughter bubbles may be systematically examined by changing capillary pressure and pore-throat geometry. Experiments show that the sizes of the daughter bubbles decrease with increasing capillary pressure following an exponential relationship [202]. The pore-throat geometry also plays a vital role in bubble breakup. An increase in the pore-throat ratio or length of the throat causes a decrease in daughter bubble sizes. As such, capillary snap-off is the predominant mechanism for bubble breakup in these pore-throat structures [202].

4.4.2. Leave-Behind

The leave-behind foam formation mechanism dominates below critical velocity in homogeneous formations [200]. Once gas invades a liquid-saturated zone, it seeps through many interconnected channels. Usually, different gas fronts seep into the same liquid-filled pores from different directions. Consequently, these fronts squeeze the liquid inside the pore into the lamella. The stability of the lamella depends on the amount of surfactant in the liquid phase. If enough surfactant is present, the lamella is stable; otherwise, it ruptures.

Leave-behind often occurs in highly connected porous media. Due to the formation of many lamellas, gas pathways are blocked, which reduces the relative permeability to the gas phase by creating dead-end pathways and blocked flow channels. This mechanism generates a relatively weak foam [200].

4.4.3. Lamella Division

The lamella division mechanism requires a moving lamella, which means some foam generation must already have occurred. Therefore, lamella division is considered a secondary foam-generation mechanism. The mechanism of lamella division is similar to the snap-off mechanism. Separate bubbles may block or flow in gas pathways, which may happen several times at any given site and become more critical at higher gas velocities. This phenomenon makes distinguishing snap-off and lamella division mechanisms challenging without a pore-level examination [200], which is possible in microfluidic systems. Microfluidic platforms provide real-time fluid injection control and enable direct visualization of foam generation, propagation, and transport. The main challenge with these platforms is their inability to withstand high-pressure conditions, which may limit observations of supercritical CO_2 foams [203].

5. Long-Term Storage, Security, Policy, and Regulations

Potential risks associated with underground CO_2 storage may be described using the following five categories [204]: (i) CO_2 leakage to the atmosphere, (ii) potential CO_2 pollution of groundwater and underground resources, (iii) induced seismicity, (iv) subsidence of the earth surface, and (v) degradation of underground storage reservoirs. CO_2 that is injected in geological formations may migrate out of the host reservoir and leak into the atmosphere/biosphere. These potential leaks depend on the reservoir's well and cap rock integrity and trapping mechanisms [205]. Although CO_2 is a non-toxic constituent of the atmosphere, high concentrations of CO_2 may pose problems. Uncontrolled leakage of large volumes of CO_2 may accumulate near the surface and cause asphyxiation and

loss of consciousness to humans in the vicinity [206,207]. In 1986, more than 1700 villagers and 3500 cattle were killed due to a significant CO_2 release from a natural underground CO_2 reservoir near Lake Nyos in Cameroon [208]. The rate of CO_2 leakage from geological reservoirs may vary, but releases/leaks of excessive amounts of CO_2 may be hazardous to the environment and human life [206].

CO_2 leaks can also contaminate groundwater (including underground sources of drinking water (USDW)), which may happen by either CO_2 directly leaking into aquifers or as a result of the brine displaced by CO_2 entering the groundwater aquifer [209]. Many groundwater sources, especially shallow ones, may be used for potable water, as well as industrial and agricultural purposes. Once CO_2 dissolves in groundwater, it forms carbonic acid, lowers the pH value, and may cause unintended effects such as the mobilization of toxic metals, chloride, and sulfate [206]. Metal contamination of groundwater can cause exposure to carcinogenic materials and harm human health. The EPA regulates the number and allowable concentrations of these inorganic contaminants. For example, 12 toxic cations, including strontium and molybdenum, were mobilized in a pilot project of the DOE [210,211]. The impact of leaked CO_2 on groundwater quality also depends its geochemical evolutionary processes, such as reaction time [212]. Another primary concern regarding CCUS is induced seismicity and leakage of CO_2 from fractures or fault slips due to the high injection pressure [213]. CO_2 injection may cause an increase in pore pressure and a reduction in effective stress, which may cause an expansion in reservoir rocks and deformation of the overburden [214]. The increased pressure and the straining of reservoir rock may cause small seismic events, which may be observed via geophones. Factors such as in situ stress, injection pressure, and the existence of fractures, amongst other rock properties, can trigger these microseismic events [215]. These microseismic events are usually observed in CO_2 storage sites or different injection operations and may be used in underground monitoring of injected fluid flow [215–217]. In the 1960s, several earthquakes between 3 and 4 Richter magnitude were observed near Denver, Colorado, due to fluid disposal operations in reservoirs. Earthquakes are directly connected with injection activities and changes in pore pressure [218].

5.1. Long-Term Storage

The geologic storage of CCUS involves various risks, including the potential endangerment of USDWs to induced seismicity. In the US, these risks are primarily addressed through Class VI permitting under the Underground Injection Control Program of the Safe Drinking Water Act. The Class VI program applies to the full lifecycle of CCUS projects: (i) site selection and characterization, (ii) operations (e.g., CO_2 injection), (iii) post-injection site care, and (iv) site closure. The Class VI program comprehensively and extensively addresses all relevant risks in those phases. According to the 2005 IPCC's Special Report on Carbon Dioxide Capture and Storage [47,219]:

"Observations from engineered and natural analogs as well as models suggest that the fraction retained in appropriately selected and managed geological reservoirs is very likely25 to exceed 99% over 100 years and is likely20 to exceed 99% over 1000 years. For well-selected, designed, and managed geological storage sites, most of the CO_2 will gradually be immobilized by various trapping mechanisms and, in that case, could be retained for up to millions of years. Because of these mechanisms, storage could become more secure over longer timeframes".

Nonetheless, the safety of long-term storage can be a concern for the public, particularly in the long-term stewardship phase of a project, which commences after a site has been closed and the Class VI program ends. These concerns may be magnified by the need to store CO_2 in the subsurface on timescales on the order of 10,000 years [220]. For optimal storage capacity, suitable reservoirs have pressure and temperature conditions that ensure CO_2 remains supercritical [110]. Injection of CO_2 in the liquid state may create cold regions around wellbores and affect long-term rock mechanical stability. Injection at the beginning of the process can also specifically damage reservoirs and caprocks. Therefore, special

attention must be paid to the first month of injection [221], and interactions among CO_2, water, and rock are important during the injection stage [222]. Busch et al. [223] studied the effect of several factors that influence caprock seal integrity for CO_2 storage. The risk of fracture generation in the reservoir and caprock is based on the production history of the reservoir, and wells pose high-potential leakage pathways. Chemical alterations affect physical properties of wellbore cement. Once CO_2 reaches the resident brine, permeability may be decreased near the front, lowering the risk of leakage in abandoned wells [224]. The pressure may be well below its fracture pressure in many depleted hydrocarbon reservoirs. Therefore, the risk of injecting CO_2 into these reservoirs is reasonably low. In contrast, for deep saline aquifers, CO_2 injection, especially at the beginning, may be closer to the fracture pressure [225].

The capillary threshold pressure, effective permeability (especially once the system pressure exceeds the threshold pressure), diffusion through water-filled pore volume, and adsorption play essential roles in cap rock/seal integrity [223]. Among potential geologic CO_2 storage sites, depleted oil and gas reservoirs are often the safest candidates because they can safely contain oil and natural gas over geological timescales [47].

5.2. CO_2 Storage Policy

The geologic storage of CO_2 has been in the commercial sphere for some time. Natural CO_2 domes, such as McElmo Dome in Colorado, are understood to have stored significant volumes of natural CO_2 over geologic time [226]. Formations such as McElmo Dome have been accessed for many decades to produce CO_2 that is used for CO_2-EOR. Meanwhile, "[t]he first carbon capture plant was proposed in 1938, and the first large-scale project to inject CO_2 into the ground launched in the Sharon Ridge oilfield in Texas in 1972. Around 24 years later, Norway launched the world's first integrated carbon capture and storage project, known as Sleipner, in the North Sea [227]".

In terms of regulations, Class II of the UIC program, which governs, in part, the injection of CO_2 for use in EOR, was implemented in the 1980s [228]. Class VI of the UIC program, which specifically applies to the injection of CO_2 in deep geologic formations unsuitable for CO_2-EOR and other productive activities, was finalized in December 2010 by the US Environmental Protection Agency (EPA) [229].

As a matter of international climate policy, the 2005 IPCC special report referenced above marked a watershed in that it reflects a consensus view of international expectations that geologic storage, if properly regulated, would be environmentally safe. Furthermore, in 2005, the 1997 Kyoto Protocol entered into force [230,231]. In particular, the Kyoto Protocol's Clean Development Mechanism considers various methodologies to implement CCUS projects to generate CO_2 credits—specifically known as Certified Emission Reductions; however, no projects were ever approved under the mechanism. CCUS is expected to play a significant role under the Paris Agreement, which replaced the Kyoto Protocol; however, the jury is still out on this matter. Numerous climate modelers have concluded that CCS is needed to achieve the Paris Agreement's goals [232–235], and several countries have indicated their intent to pursue CCUS projects to achieve their country-specific climate commitments via nationally determined commitments under the Paris Agreement [236].

For many years, Congress has implemented incentives for CCUS, including but not limited to the section 45Q tax credit for "carbon oxide sequestration" [237,238]. In 2005, DOE launched its carbon sequestration program [239]. Since then, Congress has authorized and appropriated tens of millions of dollars to the DOE to support basic research on CCUS-related technologies (e.g., capture technologies) and applied research (e.g., DOE's CarbonSAFE program). For these and other reasons, the US is the leading country in carbon capture projects, with about 13 commercial-scale carbon capture facilities with 25 million tons of annual CO_2 capture capacity as of February 2021 [240].

5.3. Well Classes and Related Regulations

Injection and abandoned wells are likely sources of CO_2 from underground reservoirs [47]. Well integrity studies categorize wells according to their purpose, such as wells used for injection and monitoring of CO_2 production and those that are abandoned [128]. In the US, state-level institutions have primacy regarding pre-existing policies for CO_2 injection. However, as noted above, the EPA's UIC Program is the main regulatory program governing injection well policy [239]. The EPA's UIC program distinguishes six different classes of injection wells based on factors such as their type and depth of injection and their potential to endanger USDW [241] (see Table 1).

Table 1. The EPA's well classes (adapted from [241]).

Well Class	Description	Examples		Requirements
Class I	Industrial and municipal waste disposal	• Petroleum refining • Metal/food/chemical production • Municipal wastewater treatment wells		• Siting • Construction • Operation/monitoring/testing • Record keeping • Closure
Class II	Oil-and-gas-related injection wells	• Disposal wells • Enhanced recovery wells • Hydrocarbon storage wells		• Construction • Operation • Monitoring and testing • Reporting • Closure
Class III	Mining solution wells	• Uranium • Salt • Copper • Sulfur mines		• Tubing/casing/cementing • Well pressure testing • Monitoring of injection pressure and flow rate • Monitoring of USDWs • Closure
Class IV	Shallow hazardous and radioactive injection wells	The EPA banned the use of these wells in 1984		
Class V	Underground injection wells of non-hazardous fluids	Shallow wells	• Stormwater drainage • Septic system leaching • Agricultural drainage	Operation of these wells is "authorized by rule", meaning that they can be operated without a permit as long as injection does not endanger USDW
		Complex Class V wells	• Aquifer storage and recovery • Geothermal electric power • Deep injection wells for salinity control	
Class VI	Geological sequestration of CO_2	Injection of CO_2 into deep geological formations		• Siting • Construction • Operation • Testing • Monitoring • Closure

Class I: This class comprises industrial and municipal waste disposal wells. This class may be used to inject hazardous and non-hazardous waste in deep, confined rock formations thousands of feet below the lowermost USDW. Examples include wells used in industrial processes such as petroleum refining; chemical, pharmaceutical, and metal production; commercial disposal; food production; and municipal wastewater treatment.

Class II: This class is meant exclusively for oil and gas production and the injection of related fluids. These fluids include brine that is produced along with oil and gas. Class II wells usually fall into three categories: disposal wells, enhanced recovery wells, and hydrocarbon storage wells.

Class III: This class is used for dissolving and extracting minerals in the mining industry. Minerals extracted with this method include uranium, salt, copper, and sulfur. In the US, more than 50 percent of salt and 80 percent of uranium extraction involve class 3 wells.

Class IV wells: This class was used to inject hazardous and radioactive waste into shallow geological formations, including USDW. The EPA banned the use of these wells in 1984.

Class V: These wells are used for the injection of non-hazardous fluids into or above USDW. Most of these are stormwater drainage wells, septic system leach fields, and agricultural drainage wells. Disposal of this water may threaten groundwater quality if not managed properly.

Class VI: The EPA distinguishes class VI wells specifically for geologic sequestration of CO_2 in deep formations. There are specific requirements for class VI wells that address siting, construction, operation, testing, monitoring, and closure. The use of these wells is not mature, and the EPA maintains an inventory of permitted class VI wells.

The EPA has delegated UIC program primacy for all injection well classes. For class VI wells, the EPA holds direct implementation authority in all states except Wyoming and North Dakota. These two states have primacy for all well classes [242].

Storage Policy in Europe

There are three main international conventions of particular relevance to the storage and transportation of CO_2 in Europe: the Basel Convention, OSPAR, and the London Convention and Protocol [243]. The Basel Convention addresses the control of transboundary movements and disposal of hazardous waste; it was adopted in 1989 in Basel, Switzerland, and entered into force in 1992 [244]. The OSPAR convention is an amendment that allows the storage of overwhelmingly pure CO_2 in subsoil geological formations with the intention of permanent storage without any adverse effects on the marine environment and human health [243,245]. In contrast to the Basel agreement, the London Convention and Protocol may represent a legal barrier to the transboundary movement of CO_2 for storage in subseabed geological formations. This protocol mainly focuses on prohibiting the dumping of waste and preventing pollution of the seas [243,246].

It is estimated that about 80% of Europe's CO_2 storage capacity is in saline aquifers [243]. The European Commission published specific guidance for implementing the CCUS directive, which contains guidelines for CO_2 storage complex characterization, the composition of the injected CO_2 stream, monitoring, and corrective measures. The guidance explicitly mentions monitoring as a critical activity for ensuring the safety of geological storage [247].

Considering all policies related to CO_2 storage, monitoring is often a crucial requirement. The main objectives of underground CO_2 storage monitoring are to ensure storage integrity, ensure safety requirements for subsurface activities during and after the operations, and ensure that the injection process occurs as planned and in the target formation [248].

6. Monitoring

Monitoring and surveillance refer to close observation of the host formation and the stored fluids. The distinction between the two is that monitoring may also comprise analysis and prediction components, making it more active in contrast with surveillance, which is more passive [249]. Monitoring in industrial systems often includes sensing, measurements, and feedback. Monitoring may also imply the presence of an alarm when system parameters exceed specific tolerances [249].

In underground CO_2 sequestration projects, monitoring usually includes monitoring, verification, and accounting, and accounting (MVA) technologies and is considered an essential part of safe, effective, and permanent geologic CO_2 storage operations. MVA technologies are typically classified as those that are meant for (i) atmospheric, (ii) near-surface, and (iii) subsurface applications related to ensuring the safety of injected CO_2 [250]. Atmospheric monitoring tools are based on measuring the density and flux of the CO_2

above CO_2 storage sites. Near-surface monitoring technology measures CO_2 between the top of the soil and the shallow groundwater zone. Subsurface monitoring technologies include reservoir depth techniques for CO_2 detection [251] (see Figure 4).
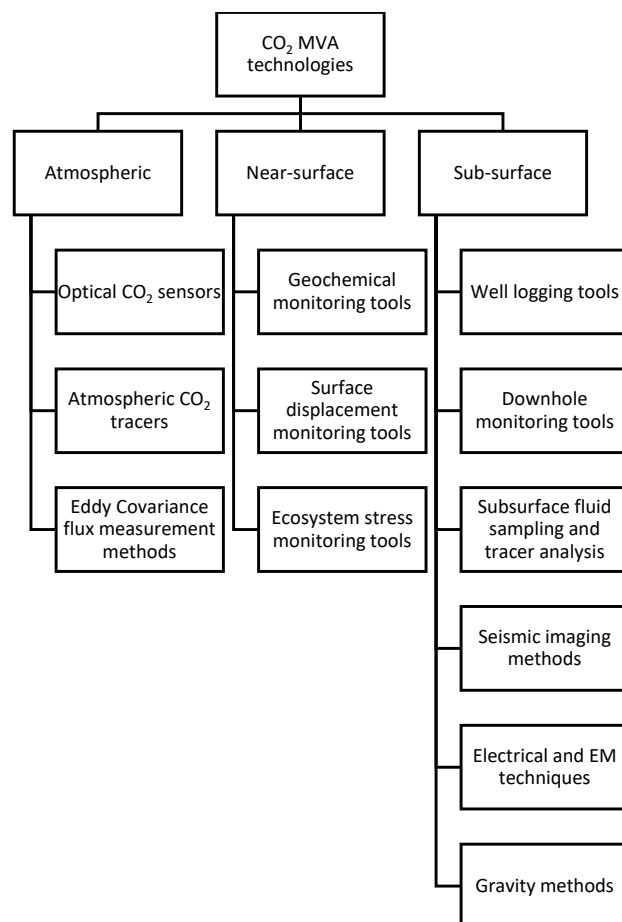

Figure 4. Various CO_2 monitoring, verification, and accounting technologies.

In general, geological CO_2 sequestration projects comprise six stages: (i) site selection and characterization, (ii) site preparation and construction, (iii) CO_2 injection operations, (iv) post-injection site care (PISC), (v) site closure, and (vi) long-term stewardship. Monitoring is critical in all these stages and, in a broader sense, includes technologies to characterize the site, plan and manage the site's construction, and perform post-closure surveillance [252,253].

In the US, monitoring requirements arise in different legal and policy contexts. These contexts include but are not limited to the following:

(i)   Monitoring to protect USDWs: Class VI regulations of the underground injection control program under the Safe Drinking Water Act impose monitoring requirements to protect USDWs.

(ii)   Monitoring for purposes of reporting CO_2 emissions in the atmosphere: EPA's GHG Reporting Program (GHGRP) requires entities engaged in specific commercial activities to report their atmospheric emissions of GHGs to enable their tabulation. Monitoring of CO_2 in geologic storage primarily arises under Subpart R.R. of the GHGRP ("Geologic Sequestration of Carbon Dioxide"). Holders of Class VI permits must report under Subpart R.R. and implement EPA-approved MVA plans [254]. Companies engaged in CO_2 EOR injection under Class II permits may opt into Subpart R.R.

(iii)   Monitoring to obtain federal tax incentives: The primary federal tax incentive for the geologic storage of CO_2 arises under section 45Q of the federal tax code (26 U.S.C. § 45Q). Credit amounts vary by activity, but the general principle is that CO_2 must be in

"secure geological storage" (see, e.g., id. § 45Q(a)(3)(B)). Via regulation, the Secretary of the Treasury has stated that to satisfy the "secure geological storage" requirement and thus be eligible to obtain the tax credit, taxpayers must either (i) report under Subpart R.R. of the GHGRP to include its M.R.V. requirement, as discussed above; or (ii) comply with ISO standard 27916 ("Carbon dioxide capture, transportation, and geological storage—Carbon dioxide storage using enhanced oil recovery (CO_2-EOR)". On 21 June 2022, the EPA proposed that taxpayers reporting under ISO standard 27916 report under a new set of GHGRP regulations, i.e., Subpart V.V. (87 Fed. Reg. 36920).

(iv) Monitoring to comply with state GHG programs: Some states—most notably California—separately regulate GHG emissions and/or the carbon content of transportation fuels under programs known as low-carbon fuel standards (LCFSs). California's LCFS, for example, explicitly recognizes the geologic storage of CO_2, provided it is conducted following a California Air Resources Board (CARB) protocol ("Carbon Capture and Sequestration Protocol under the Low Carbon Fuel Standard" [255]). CARB's CCUS protocol separately imposes a variety of CO_2 monitoring requirements.

(v) Monitoring to obtain carbon offsets. Carbon market registries—the American Carbon Registry and Verra—are advancing various methodologies enabling eligible CCUS projects to monetize their activities by creating carbon offsets. Once finalized, those methodologies will also address monitoring.

In the EU, monitoring techniques are regulated by the European Commission under the European CO_2 Storage Directive, which specifies monitoring of several mandatory items, including fugitive CO_2 emissions at the injection facility, volumetric flow of CO_2 at wellheads, CO_2 mass flow, chemical analysis of injected materials, reservoir temperature, and pressure measurements for determining CO_2 phase behavior and state. The directive requires "zero detectible leakage" before operators close the site and transfer responsibility to national authorities [247,256].

6.1. Atmospheric CO_2 Monitoring Technologies

Early atmospheric detection of CO_2 from CCUS sites is essential for taking remediation action and ensuring public safety [257]. Measurement of CO_2 concentrations at the surface is also required for safe geological CO_2 storage [257]. According to the US DOE, atmospheric CO_2 monitoring tools are classified into three main types: (i) optical CO_2 sensors, (ii) atmospheric CO_2 tracers, and (iii) eddy covariance (EC) flux measurement techniques [251].

6.1.1. Optical CO_2 Sensors

A sensor is a tool for detecting an analyte's concentration or other physical parameters over a continuous timeframe. Sensors can be classified as physical or chemical sensors depending on the source of the signal. Physical sensors detect physical properties, while chemical sensors detect signals from chemical reactions [258]. CO_2 sensors have two main types: non-dispersive infrared (NDIR) sensors and ceramic sick film gas sensors. NDIR sensors use an optical sensing principle and often have higher accuracies and long-term stability [259]. Many gases have a unique infrared adsorption signature in the 2–14 μm range. Analysis of adsorption spectra of gas or liquid mixtures allows for identification and quantification of each chemical based on its unique characteristic wavelength [260]. This primary infrared signature enables the detection of CO_2 using optical fibers to transmit light in the given range. For example, chalcogenide optical fibers can transmit light between 1 and 6 μm and are candidates for fiberoptic CO_2 sensor development [261]. Atmospheric CO_2 monitoring techniques are applied in potential CO_2 leak areas. The authors of [262] developed and tested mobile open-path laser techniques near the ground surface at a geologic CO_2 storage site. This method successfully detects significant gas venting zones. The authors of [257] developed and tested a mobile system for detecting CO_2 leaks in CCUS sites. The mobile system operates based on measuring O_2/CO_2 concentration ratios and can determine plumes with as little as 100 ppm CO_2 concentrations.

6.1.2. Atmospheric CO_2 Tracers

Chemical tracers such as SF6 are useful for subsurface monitoring of CO_2. Low concentrations of these tracers may be added to the injected CO_2 to help detect and quantify leaks. Other gases, such as CH_4 or CO from fuel or biomass combustion, may be used as atmospheric CO_2 tracers [263]. Carbon dioxide isotopologues with isotopic values different from those of many natural CO_2 sources may accompany the injected CO_2 and be used as tracers. The Otway carbon capture and storage project in Australia is the first CO_2 geological storage project with a comprehensive atmospheric monitoring program, including the use of atmospheric tracers [264]. Simulations of the Otway project show that even one micromolar concentration of SF6 added as a tracer to CO_2 can be more easily detected [265].

6.1.3. Eddy Covariance Flux Measurement Methods

The eddy covariance method allows for measurement of heat, mass, and momentum exchanges between flat, horizontally homogeneous surfaces and the overlaying atmosphere. The flux density between the surface and the atmosphere may be calculated using the covariance between turbulent vertical wind fluctuations and the quantity of interest [266]. This method may measure CO_2 fluxes above the treetops and quantify on-site CO_2 emissions [267]. The CO_2 flux measurement technique can be an open- or closed-path system [268]. Closed-path measurements can be performed by calculating the covariance between vertical windspeed and the density of CO_2 obtained from a closed-path analyzer. On the other hand, sonic anemometers are used for open-path measurements [269]. Sampling of gases with a closed-path system may cause flux losses, which may cause inconsistent flux measurements. Therefore, some corrections may be needed when using closed-path flux measurements [270]. Lewicki et al. [271] used the eddy covariance technique to detect surface CO_2 leaks from two subsurface sources. After site-specific experiments, they concluded that the eddy covariance method is a promising tool for monitoring geological carbon sequestration projects.

6.2. Near-Surface CO_2 Monitoring

Near-surface CO_2 monitoring techniques, as summarized below [250], track the near-surface presence of injected CO_2.

6.2.1. Geochemical Monitoring

Geochemical monitoring includes shallow groundwater sampling, hydrocarbon sampling, soil gas sampling, geochemical fluid sampling, reactive transport modeling, CO_2–brine–rock interactions, pore-scale mineral alteration, and modeling of CO_2 in aquifers [272]. CO_2 is usually injected with water to decrease CO_2 mobility, especially during EOR. The brine's pH value and carbon dioxide–water mixtures' acidity can vary in miscible CO_2 floods, which may dissolve carbonate minerals in the formation and cause changes in permeability [273,274]. Furthermore, during storage in saline aquifers, aqueous solutions are displaced due to the low compressibility of water. These solutions contain highly saline brine, which is considered ecologically toxic in shallow environments. Several technologies, such as pump tests, wireline sampling, sensor-based systems, and side coring, are available for geochemical monitoring in deep and shallow environments [275]. The U-tube sampling methodology developed in [276] is a convenient method for collecting large volumes of multiphase samples at in situ pressures. Zimmer et al. [277] developed a real-time geochemical monitoring tool and tested it at the CO_2SINK project in Ketzin, Germany. The tool uses a phase-separating membrane to separate dissolved gas from fluids, and the collected gases are analyzed by a mass spectrometer.

6.2.2. Surface Displacement Monitoring Tools

Subsurface deformation due to the injection or extraction of fluids can be measured using various measurement techniques such as differential global positioning systems

(DGPSs), tiltmeters, and interferometric synthetic aperture radar (InSAR) [278]. Using these techniques in the oil and gas industry has proven economical and technically effective [279].

High-resolution GPS surveys can measure surface displacement due to injection. Permanent GPS stations or monuments offer high accuracies, high temporal sampling, and accurate monitoring of surface displacements [280]. DGPS is an mm-level monitoring technique that uses a minimum of two GPS receivers and sophisticated Kalman filtering to measure horizontal and vertical motion. This system's setup requires placing one GPS receiver in an area that is expected to be relatively motionless and another receiver in the area of interest [278].

Interferometric synthetic aperture radar (InSAR) provides high-precision, large-scale, surface-based deformation results for oilfield monitoring. Currently, InSAR is a cost-effective and promising ground monitoring technology [281]. This technology is based on phase delay measurements of a radar wave or microwave to establish points of displacements on the surface of interest. Satellite-based and airborne systems may be used for mapping and have successfully measured earth surface deformations [282]. InSAR is effectively applied to the In Salah geological CO_2 storage project in Algeria. Data analysis shows that an injected mass of 3 million tons of CO_2 resulted in 5 mm of surface displacement per year [283]. Satellite images usually cover 2500–10,000 square km, which may be adequate to cover multiple CCUS project areas [278].

Tiltmeters are instruments that work based on a highly sensitive electrolytic bubble level. A high-tech carpenter's level can measure movements of lilt as small as one nanoradian. These tools can be deployed in surface arrays on wellbores to map fracture height and other parameters. During CCUS projects, surface arrays are usually applied to collect intensive data that are often processed through a geomechanical inversion [278].

6.2.3. Ecosystem Stress Monitoring Tools

Elevated levels of CO_2 may induce changes in the soil that stress the vegetation. Therefore, vegetative stress level measurements may indicate a CO_2 leak at geologic CO_2 storage sites. Tools such as aerial photography, satellite imagery, spectral imagery, and known baseline regional information may detect vegetative stress. Spectral images of vegetation reveal changes in the light reflectance of leaves, which correlate with CO_2 levels in the soil [250].

6.3. Subsurface CO_2 Monitoring

Subsurface monitoring is explicitly required under Class VI to protect USDWs [284]. The main objectives of subsurface CO_2 monitoring include monitoring of the evolution of the dense-phase CO_2 plume, assessment of high-pressure areas caused by injection, and determination of the limit of pressure and CO_2 migration paths within acceptable areas of the reservoir. The main subsurface CO_2 monitoring tools are discussed below [250].

6.3.1. Well Logging

Wireline logging is a technique that covers a wide array of measurements by trolling a sonde through the wellbore and obtaining continuous data on the surface from the sensors. Some of the most common wireline logs include gamma-ray density, formation resistivity, temperature and pressure, self-potential, acoustic velocity, and new and sophisticated tools such as formation microimages (FMI) and those that use nuclear magnetic resonance (NMR) [285].

In previous studies, injected CO_2 was successfully monitored using standard oilfield tools. The authors of [286] developed a technique for monitoring miscible CO_2 flooding in fiberglass-cased wells with wireline logs. Three-phase saturation (oil, CO_2, and water) was monitored using resistivity and neutron logs. The authors of [287] used pulsed neutron logs to monitor CO_2 sequestration in saline aquifers. The results explain how the migration and accumulation of CO_2 occur in reservoirs by quantifying fluid saturations within the reservoir [287]. Neutron logs yield porosity data and are responsive to the amount of

hydrogen associated with the water in the formation. During CO_2 injection, neutron porosity decreases, and using the ratio of change between baseline data and each log data point helps to determine CO_2 saturation [288]. Xue et al. [289] used induction, sonic, and neutron logging tools to determine CO_2 breakthrough in Japan's Nagaoka geologic CO_2 sequestration pilot site. Sonic and neutron logs show similar but superior CO_2 distribution data compared to induction logs. Estimation of CO_2 saturation values is based on measuring reductions in sonic or P-wave velocities and increases in resistivity [289]. Sonic logs may acquire P- and S-wave velocities. Small amounts of CO_2 present in the formation may result in drastic P-wave velocity reductions because of the sensitivity of P-waves to propagation speed differences between water and CO_2 [288]. Sakurai et al. [290] used a pulsed neutron tool to monitor saturation through thermal neutron absorption cross-section changes. The significant contrast of sigma values between CO_2 and water enables the estimation of water and CO_2 saturations. Despite the availability of these tools, it is rather challenging to determine CO_2 saturation values deep in formations [285].

6.3.2. Downhole Monitoring Tools

Temperature and pressure measurements constitute fundamental monitoring parameters for CO_2 injection. During injection, reservoir pressure should be carefully monitored to prevent failure of the sealing formation. Piezoresistive and quartz-based deep subsurface pressure sensors have a high accuracy and a low resolution [291]. Fiber optic light-pulse-based modular borehole monitoring systems were developed to transmit electrical power signals, allowing for distributed temperature/pressure measurements and acoustic/temperature sensing (DTS) [292,293]. DST has several advantages over other temperature sensors, including its ability to measure continuous temperature profiles with high temporal and spatial resolution under various conditions [294]. DST monitoring usually starts with well completion and may provide hints about cement quality during the cementation process, in addition to allowing for in situ measurements of the heat transfer capacity of CO_2, formation fluids, and reservoir rock [295].

6.3.3. Subsurface Fluid Sampling and Tracer Analysis

There are several in situ fluid sampling technologies available. A cased hole dynamics tester (CHDT) was used to collect fluid samples from observation wells at Japan's Nagaoka pilot site [296]. Developed by Schlumberger and the Gas Research Institute, CHDTs penetrate casing, perform pressure tests, and sample and reseal the pierced hole [297]. The MDT modular formation dynamic tester is another well-known tool developed by Schlumberger, that performs pre-CO_2 injection sampling. However, its use is not operationally feasible during the active injection process [285].

Quadrupole mass spectrometry (QMS) allows for real-time analysis of CO_2 and CH_4. The authors of [276] developed a U-tube sampling system to collect multiphase fluid samples at in situ pressures. It was initially tested to monitor the Frio CO_2 sequestration project in Liberty County, TX. The U-tube sampling system comprises a small-diameter tube that goes down to the bottomhole and returns the sample to the surface. Applying compressed gas to one leg (drive leg) of the tube causes the check valve to close and forces the fluid sample to be recovered with the sample tube on the surface.

Another way to monitor CO_2 injection in downholes is tracer analysis. Chemical tracers are widely used for tracing the movement or interaction of gases, liquids, or solids in environments that are otherwise physically difficult to access. Although the main benefit of using tracers is understanding the transportation and dispersion of materials through a system, they can also provide information about the physical and chemical properties of the system. Tracer application areas include geochemistry, biochemistry, and marine and environmental chemistry [298]. For example, stable carbon gas isotopes may serve as natural tracers for the mapping of reservoir heterogeneities and reservoir architecture in petroleum systems [299]. Superparamagnetic iron oxide nanoparticles may act as tracers in medicine to obtain high-contrast tomographic images of the human

body [300]. Hassoun et al. [301] developed a method for underground leak detection inside a buried pipe involving perfluorocarbon tracers at a part-per-trillion (ppt) level. Commonly used tracers in the oil and gas industry include radioactively tagged molecules such as tritiated hydrogen, methane, and 85 Kr. The main reason for using radioactive molecules is their detectability at low concentrations [302]. The improvement of new analytical detection methods has enabled the use of other non-radioactive molecules as tracers [299,302,303]. Tracer data provide an improved understanding of reservoir fluid/gas interactions. Tomich et al. [304] developed a technique using ethyl acetate as a tracer for determining residual oil saturations in hydrocarbon reservoirs. Tracers used for surveillance may be classified based on their radioactivity [249] (see Figure 5).
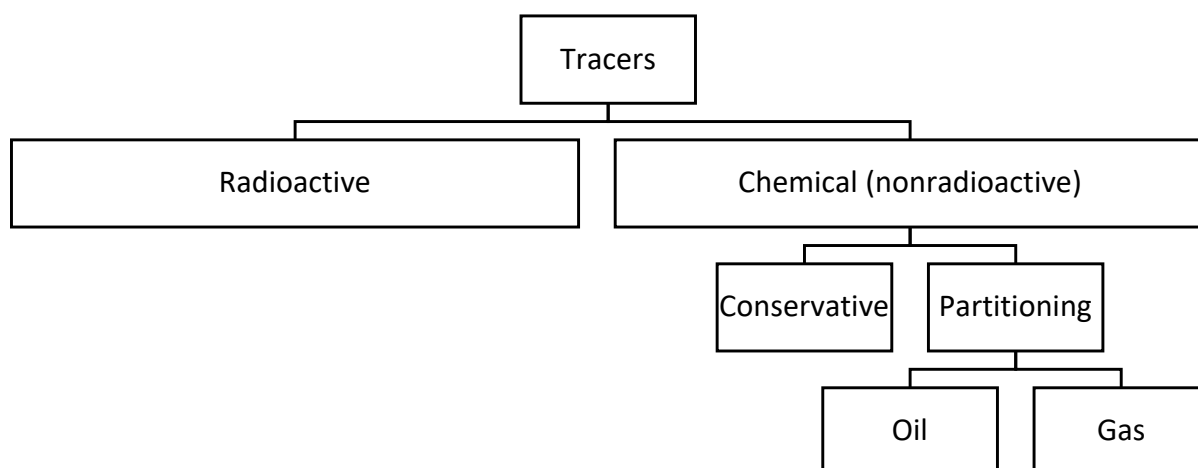

Figure 5. Tracers for CO_2 monitoring.

Conservative tracers move with aqueous fluids, while partitioning tracers move and interact in and out of both phases. Tracers may be classified as single-well and interwell tracers [249]. Single-well tracers are an accurate way to determine residual oil saturations due to their ability to estimate large reservoir areas regardless of porosity [305]. Interwell tracers provide information about flood patterns within a reservoir. Although the collected data are often reliable and unambiguous, the interwell tracing method may be time-consuming (from several days up to months), as the tracers may take a long time to reach the producers from injection wells [306]. Tracers should be chemically inert, non-toxic and environmentally safe, persistent, and stable for the period of the monitoring process at low volumes and cost [307]. It is often more straightforward and cost-effective (and therefore preferable) to inject limited amounts of tracers than to inject them continuously over long periods [298]. Examples include slugs of perfluorocarbon tracers used in the West Pearl Queen CO_2 sequestration pilot test site in SE New Mexico [308]. Perfluorocarbon tracers are common in CO_2 sequestration projects. These tracers were used to monitor a CO_2 injection project in the Dutch part of the North Sea [309]. Moreover, noble gases such as xenon, helium, argon, and neon may be used as tracers for CCUS, mainly because they are chemically inert and environmentally safe [307].

6.3.4. Seismic Imaging

CO_2 significantly affects seismic data regarding both seismic amplitudes and velocity pushdown effects [248]. Seismic monitoring of Sleipner geological CO_2 storage in saline aquifers showed that time-lapse seismic surveying might be a suitable geophysical monitoring technique. Borehole vertical seismic profile (VSP) and crosswell data from the Frio pilot geological CO_2 sequestration project demonstrated the usage of seismic imaging for plume migration monitoring and the cost-effectiveness of using permanent sensors in long-term plume migration studies [310]. Tests of the permanent sensors yielded high-quality subsurface images from the Penn West CO_2 injection pilot test in Canada [285,311].

Crosswell seismic imaging provides high-resolution tomographic images between two wells [285]. Crosswell seismic tomography in Japan's Nagaoka pilot project shows that injected CO_2 can be observed as velocity reduction areas. Increasing the injected CO_2 amount results in higher velocity reductions on tomograms [312]. Moreover, interpreting the reflection seismic sections in crosswell data may inform flow patterns. Crosswell seismic imaging may also be used to augment 4D monitoring applications [313].

Four-dimensional seismic interpretation technologies are helpful for reservoir and injection monitoring [314]. Four-dimensional seismic technology is composed of repeated three-dimensional seismic surveys over a time period. These timelapse measurements should ideally capture changes in seismic signals as changes in reservoir or fluid properties [249]. At least two 3D seismic surveys and a set of initial baseline surveys are needed for 4D seismic technology. The baseline survey is conducted before CO_2 injection starts, and follow-up surveys should be conducted after a few years of sequestration [315]. Chadwick et al. [316] demonstrated that time-lapse 4D seismic monitoring is a valuable tool for determining in situ CO_2 amounts. Three-dimensional seismic data were acquired from the Sleipner field in 1999 and 2001 [316]. The main seismic attributes used for seismic interpretations are amplitude, impedance, root mean square (RMS), and sweetness [317]. Generally, CO_2-saturated reservoirs have a considerably greater impedance in brine-saturated rocks than in oil-saturated regions [315].

Certain seismic waves, referred to as Krauklis waves, can constrain fracture geometry. The waves resonate within the fluid-filled fractures at specific frequencies [318]. This resonance emits seismic signals with a signature frequency. Seismic body waves strongly depend on this resonance, which helps to distinguish Krauklis wave-related signals via seismograms [319]. Both S and P waves (body waves) can initiate Krauklis waves at the tips of fractures since the initiated waves are functions of the incident angle and the wave mode. Krauklis waves initiated by S waves have larger amplitudes and carry more information about fracture density and fluid content orientation. Therefore, Krauklis waves may be used to detect reservoir discontinuities [320,321]. Krauklis waves are a source of information in CO_2 sequestration, fractured hydrocarbon reservoirs, volcanic eruptions, and geothermal systems with different fluid-bearing rocks [321,322]. The Energy & Environmental Research Center (EERC) at the University of North Dakota and its partners developed a new CCUS MVA technology that employs Krauklis and other guided waves. This technology uses wellhead-mounted wave sources and receivers, and waveforms are tracked before and after CO_2 injection to observe the injected CO_2 until breakthrough. This technology is cost-effective for CO_2 monitoring and can provide temporal and spatial data for monitoring of CO_2 distribution within the reservoir [323].

6.3.5. Electrical and Electromagnetic (EM) Techniques

Electrical and EM techniques are based on measuring electrical or magnetic fields generated by electrodes or inductive sources. Electrical techniques are also known as electrical resistivity techniques and use lower frequencies than EM techniques [324]. Electrical resistance tomography (ERT) is an electrical measurement technique for indirectly visualizing fluid movements in the subsurface. This technique requires an intermediate inversion algorithm to convert raw electrical resistance measurements to tomographic images of a fluid plume [325]. The concept of ERT is to image the resistivity distribution between two boreholes using several electrodes. The electrodes are placed in these holes and are in contact with the formation. Two electrodes are loaded by known currents, and other pairs of electrodes measure the resulting voltage differences. The process is repeated between different pairs of electrodes until all linearly independent combinations are used [326]. ERT has applications in underground CO_2 storage monitoring. Karhunen et al. [327] applied ERT for 3D imaging of concrete. Ramirez et al. [328] used ERT for mapping underground steam flood distribution. ERT was applied in CO_2 monitoring in a saline aquifer project at the CO_2SINK test site in Ketzin, Germany. Results from models and laboratory studies show its effectiveness in detecting changes in CO_2 saturation [329]. A technical long-term

behavior analysis reported that the ERT downhole permanent system is promising for the application in underground CO_2 monitoring [330].

Electromagnetic methods are another promising method with potential use in underground CO_2 monitoring similar to ERT. Due to the contrast between the electrical properties of supercritical CO_2 and brine, CO_2 saturation can be imaged [331]. Electromagnetic induction (EMI) is the operating principle. Frequency-domain EMI systems generate alternating currents at fixed frequencies, which generate primary magnetic fields when passing through a coil called the transmitter. These primary magnetic fields generate secondary magnetic fields when they pass through conductive surfaces, and a secondary coil (receiver) receives these secondary signals. Measurements can relate increasing quadrature components between fields and the apparent electrical conductivity of the subsurface [332]. Geophysical modeling of the subsurface from electrical or EM data is an inverse modeling process whereby physical property distribution of the system is calculated from measured parameters [324]. Inversion methods have been tried for EMI measurements. For example, Ayani et al. [333] developed a stochastic inversion method for monitoring CO_2 injection and migration using controlled source electromagnetic (CSEM) data.

6.3.6. Gravity Methods

The gravity method is a geophysical technique used in oil and gas exploration [334]. Gravity methods or gravimetry help to monitor density changes in CO_2 sequestration sites. They can also represent a low-cost alternative to other seismic measurements [335]. The drawbacks of gravity methods limit their application to shallow depths [336]. Similar to other potential approaches, gravity decreases as the distance between the source and the measurement point increases, which makes it difficult to detect small changes in the reservoir with traditional gravity methods [337]. The gravity method was used in the Sleipner project between 2002 and 2005 to determine in situ CO_2 densities. Considerable gravity anomalies were determined with some uncertainty. However, these measurements were based on density differences between the injected supercritical CO_2 and the aquifer brine. Continuous microgravity recordings may improve the accuracy of gravity monitoring compared with conventional time-lapsed monitoring. The increased resolution of the data may benefit analysis of the reservoir properties [338].

6.4. Emerging CO_2 Monitoring Technologies

Emerging wireless electronic technologies may be a potential future direction for CO_2 monitoring. A group of engineers and researchers from Sandia National Laboratories developed glitter-sized CO_2 sensors. These sensors can be embedded in concrete around boreholes below and above the caprock. Sensors are powered by a smart collar, which emits energy at a specific radio frequency and collects data on the amount of CO_2 in the surrounding environment. Data are sent to the collar using a different frequency, and operators receive the information at the surface. According to the researchers, a smart collar device must work for around 20 to 40 years [339,340].

Near-surface and surface CO_2 monitoring technologies are also emerging. A group of researchers from the University of Wyoming developed and tested a soil gas monitoring system in the Wyoming CarbonSAFE project near Gillette, Wyoming. The portable tool has hardware and software components, which collect data from CO_2 sensors every hour, which are transmitted to a web application. Solar panels may recharge smart battery systems, and multiple tools may be installed in an array in the monitored area. Initial tests generated encouraging results from the Wyoming CarbonSAFE project. The system is scheduled to remain in place for two years before expanding and becoming part of the long-term monitoring project [341].

The recent development of machine learning and its application in various fields may also contribute to developing existing monitoring technologies. Another group of researchers from Texas A&M University developed an unsupervised-learning-based method to analyze sensor-based data from geological storage sites and to rapidly predict the move-

ment of CO_2 plumes. This model does not rely on a geological model and may be applied to crosswell seismic tomography data [342].

Quantum technology, particularly atom interferometry-based gravity sensors, provides sensitive gravity measurements. Gravity sensing is a passive measurement method and may provide direct density measurements. These technologies hold promise for CCUS monitoring [343]. Timelapse gravity measurements performed for the Sleipner project showed that gravity might be measured in shallow seabed environments with a relatively low uncertainty, even in the presence of high levels of noise. The measurements helped characterize aquifers and estimate in situ CO_2 density values. However, because this method measures density contrasts between the aquifer fluid and the injected CO_2, applicability is limited to fluid-filled reservoirs [336].

7. Conclusions

Although CCUS is a necessary and attractive way to mitigate greenhouse gas emissions and prevent global warming, CCUS projects are often confronted with technical and non-technical challenges, including low technology readiness levels (TRL) and scale-up of capture and utilization. Over a century of experience in the oil and gas industry provides insight relevant to CO_2 storage, especially in depleted oil and gas reservoirs. However, long-term safety in CCUS remains a primary concern, which requires the development of MVA technologies and detailed monitoring plans for CO_2 sequestration projects. Non-technical issues related to policy and regulations are another consideration in deploying CCUS at scale. Potential non-technical obstacles in the US include permitting Class VI wells for CO_2 injection, complex business agreements with land and pore-space owners, and long-term liability. Despite these challenges, CCUS continues to emerge as a promising pathway to mitigate greenhouse gas emissions and provide a path to enable the transition to a net-zero emissions economy by 2050 [344].

This work provides an overview of the current state of carbon capture, utilization, and storage technologies. This paper identifies technical and non-technical areas that require additional research and government attention. Those include enhancing subsurface storage capacity in existing formations; long-term storage safety; and concomitant advancements in law, governance, and monitoring that may aid or hinder implementation. This paper reviews potential solutions for this purpose, namely the use of CO_2 foams to enhance storage capacity in depleted hydrocarbon reservoirs and their potential application for carbon storage in different formations.

References

1. Wolff, E.; Fung, I.; Hoskins, B.; Mitchell, J.F.B.; Palmer, T.; Santer, B.; Shepherd, J.; Shine, K.; Solomon, S.; Trenberth, K.; et al. Climate Change: Evidence & Causes—Update 2020. In *The Royal Society and the U.S. National Academy of Sciences*; The National Academies Press: Washington, DC, USA, 2020.
2. National Academy of Sciences. *Climate Change: Evidence and Causes: Update 2020*; The National Academies Press: Washington, DC, USA, 2020. [CrossRef]

3. US EPA. Causes of Climate Change. [Overviews and Factsheets]. 19 August 2022. Available online: https://www.epa.gov/climatechange-science/causes-climate-change (accessed on 29 March 2023).

4. US EPA. Overview of Greenhouse Gases. 16 May 2022. Available online: https://www.epa.gov/ghgemissions/overview-greenhouse-gases (accessed on 29 March 2023).

5. EIA. Greenhouse Gases—U.S. Energy Information Administration (EIA). 2021. Available online: https://www.eia.gov/energyexplained/energy-and-the-environment/greenhouse-gases.php (accessed on 29 March 2023).

6. C2ES. Global Anthropogenic GHG Emissions by Gas. 2005. Available online: https://www.c2es.org/content/international-emissions/ (accessed on 29 March 2023).

7. Pachauri, R.K.; Mayer, L.; Intergovernmental Panel on Climate Change (Eds.) Climate change 2014: Synthesis report. In *Intergovernmental Panel on Climate Change*; IPCC: Geneva, Switzerland, 2015.

8. Rahman, F.A.; Aziz, M.M.A.; Saidur, R.; Bakar, W.A.W.A.; Hainin, M.R.; Putrajaya, R.; Hassan, N.A. Pollution to solution: Capture and sequestration of carbon dioxide (CO_2) and its utilization as a renewable energy source for a sustainable future. *Renew. Sustain. Energy Rev.* **2017**, *71*, 112–126. [CrossRef]

9. NOAA Global Monitoring Laboratories. Trends in Atmospheric Carbon Dioxide. Carbon Cycle Greenhouse Gases. 22 October 2022. Available online: https://gml.noaa.gov/ccgg/trends/ (accessed on 29 March 2023).

10. U.S. Energy Information Administration (EIA). Where Greenhouse Gases Come from, Energy and the Environment Explained. 24 June 2022. Available online: https://www.eia.gov/energyexplained/energy-and-the-environment/where-greenhouse-gases-come-from.php (accessed on 29 March 2023).

11. Global Energy Review: CO_2 Emissions in 2021. 2021. Available online: https://www.iea.org/reports/global-energy-review-co2-emissions-in-2021-2 (accessed on 29 March 2023).

12. Gür, T.M. Carbon Dioxide Emissions, Capture, Storage and Utilization: Review of Materials, Processes and Technologies. *Prog. Energy Combust. Sci.* **2022**, *89*, 100965. [CrossRef]

13. Yan, J.; Zhang, Z. Carbon Capture, Utilization and Storage (CCUS). *Appl. Energy* **2019**, *235*, 1289–1299. [CrossRef]

14. UNFCCC. The Paris Agreement | UNFCCC. 2020. Available online: https://unfccc.int/process-and-meetings/the-paris-agreement/the-paris-agreement (accessed on 29 March 2023).

15. Paris Agreement. *Report of the Conference of the Parties to the United Nations Framework Convention on Climate Change*, (21st Session, 2015: Paris). Retrieved December, HeinOnline, 2015.

16. IPCC. *Climate Change and Land: An IPCC Special Report on Climate Change, Desertification, Land Degradation, Sustainable Land Management, Food Security, and Greenhouse Gas Fluxes in Terrestrial Ecosystems*; IPCC: Ginevra, Switzerland, 2019.

17. IEA. *Net Zero by 2050—A Roadmap for the Global Energy Sector*; National Academies Press: Washington, DC, USA, 2021; p. 224.

18. Solomon, B.D.; Krishna, K. The coming sustainable energy transition: History, strategies, and outlook. *Energy Policy* **2011**, *39*, 7422–7431. [CrossRef]

19. IRENA. *Global Renewables Outlook: Energy Transformation 2050*; IRENA: Bonn, Germany, 2020.

20. IEA. *Key World Energy Statistics 2021*; International Energy Agency: Paris, France, 2021.

21. IEA. *Global Energy Review 2021*; International Energy Agency: Paris, France, 2021.

22. IRENA. *Power System Flexibility for the Energy Transition, Part 1: Overview for Policy Makers*; International Renewable Energy Agency: Bonn, Germany, 2018. Available online: https://www.irena.org/-/media/Files/IRENA/Agency/Publication/2018/Nov/IRENA_Power_system_flexibility_1_2018.pdf (accessed on 29 March 2023).

23. Zheng, H.; Song, M.; Shen, Z. The evolution of renewable energy and its impact on carbon reduction in China. *Energy* **2021**, *237*, 121639. [CrossRef]

24. EIA. Country Analysis Executive Summary: China (p. 18). U.S. Energy Information Administration. 2020. Available online: https://www.eia.gov/international/content/analysis/countries_long/China/china.pdf (accessed on 29 March 2023).

25. IRENA. Country Rankings. /Statistics/View-Data-by-Topic/Capacity-and-Generation/Country-Rankings. 2022. Available online: https://www.irena.org/Statistics/View-Data-by-Topic/Capacity-and-Generation/Country-Rankings (accessed on 29 March 2023).

26. ENERGY.GOV, Renewable Energy. Energy.Gov. 2022. Available online: https://www.energy.gov/eere/renewable-energy (accessed on 29 March 2023).

27. European Commission. A European Green Deal. European Commission—European Commission. 2022. Available online: https://ec.europa.eu/info/strategy/priorities-2019-2024/european-green-deal_en (accessed on 29 March 2023).

28. Mathiesen, B.V.; Lund, H.; Connolly, D.; Wenzel, H.; Østergaard, P.A.; Möller, B.; Nielsen, S.; Ridjan, I.; Karnøe, P.; Sperling, K.; et al. Smart Energy Systems for coherent 100% renewable energy and transport solutions. *Appl. Energy* **2015**, *145*, 139–154. [CrossRef]

29. Dominković, D.F.; Bačeković, I.; Pedersen, A.S.; Krajačić, G. The future of transportation in sustainable energy systems: Opportunities and barriers in a clean energy transition. *Renew. Sustain. Energy Rev.* **2018**, *82*, 1823–1838. [CrossRef]

30. Wilberforce, T.; Baroutaji, A.; Soudan, B.; Al-Alami, A.H.; Olabi, A.G. Outlook of carbon capture technology and challenges. *Sci. Total Environ.* **2019**, *657*, 56–72. [CrossRef]

31. Yang, L.; Zhang, X.; McAlinden, K.J. The effect of trust on people's acceptance of CCS (carbon capture and storage) technologies: Evidence from a survey in the People's Republic of China. *Energy* **2016**, *96*, 69–79. [CrossRef]

32. Hasan, M.F.; First, E.L.; Boukouvala, F.; Floudas, C.A. A multi-scale framework for CO₂ capture, utilization, and sequestration: CCUS and CCU. *Comput. Chem. Eng.* **2015**, *81*, 2–21. [CrossRef]

33. IEA. *Energy Technology Perspectives 2017: Catalysing Energy Technology Transformations*; OECD: Paris, France, 2017.

34. Leonzio, G.; Bogle, D.; Foscolo, P.U.; Zondervan, E. Optimization of CCUS supply chains in the UK: A strategic role for emissions reduction. *Chem. Eng. Res. Des.* **2020**, *155*, 211–228. [CrossRef]

35. DOE. Carbon Storage Atlas: Fifth Edition. 2015. Available online: https://www.netl.doe.gov/sites/default/files/2018-10/ATLAS-V-2015.pdf (accessed on 29 March 2023).

36. IEA. Carbon Capture, Utilisation and Storage—Fuels & Technologies. IEA. September 2021. Available online: https://www.iea.org/fuels-and-technologies/carbon-capture-utilisation-and-storage (accessed on 29 March 2023).

37. Liu, H.J.; Were, P.; Li, Q.; Gou, Y.; Hou, Z. Worldwide Status of CCUS Technologies and Their Development and Challenges in China. *Geofluids* **2017**, *2017*. [CrossRef]

38. IEA. Direct Air Capture—Analysis. 2021. Available online: https://www.iea.org/reports/direct-air-capture (accessed on 29 March 2023).

39. MacDowell, N.; Florin, N.; Buchard, A.; Hallett, J.; Galindo, A.; Jackson, G.; Adjiman, C.S.; Williams, C.K.; Shah, N.; Fennell, P. An overview of CO₂ capture technologies. *Energy Environ. Sci.* **2010**, *3*, 1645–1669. [CrossRef]

40. Climate Works. Orca Is Climeworks' New Large-Scale Carbon Dioxide Removal Plant. 2021. Available online: https://climeworks.com/roadmap/orca (accessed on 29 March 2023).

41. DOE. Pre-Combustion Carbon Capture Research. Available online: https://www.energy.gov/fecm/science-innovation/carbon-capture-and-storage-research/carbon-capture-rd/pre-combustion-carbon (accessed on 29 March 2023).

42. Theo, W.L.; Lim, J.S.; Hashim, H.; Mustaffa, A.A.; Ho, W.S. Review of pre-combustion capture and ionic liquid in carbon capture and storage. *Appl. Energy* **2016**, *183*, 1633–1663. [CrossRef]

43. Wall, T.F. Combustion processes for carbon capture. *Proc. Combust. Inst.* **2007**, *31*, 31–47. [CrossRef]

44. Jansen, D.; Gazzani, M.; Manzolini, G.; van Dijk, E.; Carbo, M. Pre-combustion CO₂ capture. *Int. J. Greenh. Gas Control* **2015**, *40*, 167–187. [CrossRef]

45. Wang, M.; Lawal, A.; Stephenson, P.; Sidders, J.; Ramshaw, C. Post-combustion CO₂ capture with chemical absorption: A state-of-the-art review. *Chem. Eng. Res. Des.* **2011**, *89*, 1609–1624. [CrossRef]

46. Zhao, Z.; Cui, X.; Ma, J.; Li, R. Adsorption of carbon dioxide on alkali-modified zeolite 13X adsorbents. *Int. J. Greenh. Gas Control* **2007**, *1*, 355–359. [CrossRef]

47. IPCC. Carbon Dioxide Capture and Storage. IPCC. 2005. Available online: https://www.ipcc.ch/report/carbon-dioxide-capture-and-storage/ (accessed on 29 March 2023).

48. Bui, M.; Adjiman, C.S.; Bardow, A.; Anthony, E.J.; Boston, A.; Brown, S.; Fennell, P.S.; Fuss, S.; Galindo, A.; Hackett, L.A.; et al. Carbon capture and storage (CCS): The way forward. *Energy Environ. Sci.* **2018**, *11*, 1062–1176. [CrossRef]

49. Gibbins, J.; Chalmers, H. Carbon capture and storage. *Energy Policy* **2008**, *36*, 4317–4322. [CrossRef]

50. Stanger, R.; Wall, T.; Spörl, R.; Paneru, M.; Grathwohl, S.; Weidmann, M.; Scheffknecht, G.; McDonald, D.; Myöhänen, K.; Ritvanen, J.; et al. Oxyfuel combustion for CO₂ capture in power plants. *Int. J. Greenh. Gas Control* **2015**, *40*, 55–125. [CrossRef]

51. Koohestanian, E.; Shahraki, F. Review on principles, recent progress, and future challenges for oxy-fuel combustion CO₂ capture using compression and purification unit. *J. Environ. Chem. Eng.* **2021**, *9*, 105777. [CrossRef]

52. Soundararajan, R.; Gundersen, T.; Ditaranto, M. Oxy-combustion coal based power plants: Study of operating pressure, oxygen purity and downstream purification parameters. *Chem. Eng. Trans.* **2014**, *39*, 229–234. [CrossRef]

53. Hong, J.; Chaudhry, G.; Brisson, J.; Field, R.; Gazzino, M.; Ghoniem, A.F. Analysis of oxy-fuel combustion power cycle utilizing a pressurized coal combustor. *Energy* **2009**, *34*, 1332–1340. [CrossRef]

54. Darde, A.; Prabhakar, R.; Tranier, J.-P.; Perrin, N. Air separation and flue gas compression and purification units for oxy-coal combustion systems. *Energy Procedia* **2009**, *1*, 527–534. [CrossRef]

55. Smit, B.; Park, A.-H.A.; Gadikota, G. The Grand Challenges in Carbon Capture, Utilization, and Storage. *Front. Energy Res.* **2014**, *2*. [CrossRef]

56. Baena-Moreno, F.M.; Rodríguez-Galán, M.; Vega, F.; Alonso-Fariñas, B.; Vilches Arenas, L.F.; Navarrete, B. Carbon capture and utilization technologies: A literature review and recent advances. *Energy Sources Part A Recovery Util. Environ. Eff.* **2019**, *41*, 1403–1433. [CrossRef]

57. Coddington, K.; Gellici, J.; Hilton, R.; Wade, S.; Ali, S.; Berger, A.; Carr, M.; Eames, F.; Godec, M.; Harju, J.; et al. CO₂ BUILDING BLOCKS Assessing CO₂ Utilization Options. National Coal Council. 2016. Available online: https://www.nationalcoalcouncil.org/studies/2016/NCC-CO2-Building-Block-FINAL-Report.pdf (accessed on 29 March 2023).

58. Zhang, Z.; Pan, S.-Y.; Li, H.; Cai, J.; Olabi, A.G.; Anthony, E.J.; Manovic, V. Recent advances in carbon dioxide utilization. *Renew. Sustain. Energy Rev.* **2020**, *125*, 109799. [CrossRef]

59. National Academies of Sciences, Engineering, and Medicine. *Carbon Dioxide Utilization Markets and Infrastructure: Status and Opportunities: A First Report*; National Academies Press: Washington, DC, USA, 2022; p. 26703. [CrossRef]

60. Steinberg, M. Synthetic carbonaceous fuels and feedstocks from oxides of carbon and nuclear power. *Fuel* **1978**, *57*, 460–468. [CrossRef]

61. Meunier, N.; Chauvy, R.; Mouhoubi, S.; Thomas, D.; De Weireld, G. Alternative production of methanol from industrial CO₂. *Renew. Energy* **2020**, *146*, 1192–1203. [CrossRef]

62. Pontzen, F.; Liebner, W.; Gronemann, V.; Rothaemel, M.; Ahlers, B. CO$_2$-based methanol and DME—Efficient technologies for industrial scale production. *Catal. Today* **2011**, *171*, 242–250. [CrossRef]

63. Olah, G.A. Beyond Oil and Gas: The Methanol Economy. *Angew. Chem. Int. Ed.* **2005**, *44*, 2636–2639. [CrossRef]

64. Lü, Y.-J.; Yan, W.-J.; Hu, S.-H.; Wang, B.-W. Hydrogen production by methanol decomposition using gliding arc gas discharge. *J. Fuel Chem. Technol.* **2012**, *40*, 698–706. [CrossRef]

65. Dalena, F.; Senatore, A.; Marino, A.; Gordano, A.; Basile, M.; Basile, A. Methanol Production and Applications: An Overview. In *Methanol*; Elsevier: Amsterdam, The Netherlands, 2018; pp. 3–28. [CrossRef]

66. Bertau, M.; Offermanns, H.; Plass, L.; Schmidt, F.; Wernicke, H.-J. (Eds.) *Methanol: The Basic Chemical and Energy Feedstock of the Future*; Springer: Berlin/Heidelberg, Germany, 2014. [CrossRef]

67. Driver, J.G.; Owen, R.E.; Makanyire, T.; Lake, J.A.; McGregor, J.; Styring, P. Blue Urea: Fertilizer With Reduced Environmental Impact. *Front. Energy Res.* **2019**, *7*, 88. [CrossRef]

68. Koohestanian, E.; Sadeghi, J.; Mohebbi-Kalhori, D.; Shahraki, F.; Samimi, A. A novel process for CO$_2$ capture from the flue gases to produce urea and ammonia. *Energy* **2018**, *144*, 279–285. [CrossRef]

69. Li, W.; Shi, Y.; Zhu, D.; Wang, W.; Liu, H.; Li, J.; Shi, N.; Ma, L.; Fu, S. Fine root biomass and morphology in a temperate forest are influenced more by the nitrogen treatment approach than the rate. *Ecol. Indic.* **2021**, *130*, 108031. [CrossRef]

70. Yang, Y.; Chen, X.; Liu, L.; Li, T.; Dou, Y.; Qiao, J.; Wang, Y.; An, S.; Chang, S.X. Nitrogen fertilization weakens the linkage between soil carbon and microbial diversity: A global meta-analysis. *Glob. Chang. Biol.* **2022**, *28*, 6446–6461. [CrossRef]

71. Yang, Y.; Li, T.; Pokharel, P.; Liu, L.; Qiao, J.; Wang, Y.; An, S.; Chang, S.X. Global effects on soil respiration and its temperature sensitivity depend on nitrogen addition rate. *Soil Biol. Biochem.* **2022**, *174*, 108814. [CrossRef]

72. Hao, C.; Wang, S.; Li, M.; Kang, L.; Ma, X. Hydrogenation of CO$_2$ to formic acid on supported ruthenium catalysts. *Catal. Today* **2011**, *160*, 184–190. [CrossRef]

73. Bulushev, D.A.; Ross, J.R.H. Towards Sustainable Production of Formic Acid. *ChemSusChem* **2018**, *11*, 821–836. [CrossRef] [PubMed]

74. Sternberg, A.; Jens, C.M.; Bardow, A. Life cycle assessment of CO$_2$-based C1-chemicals. *Green Chem.* **2017**, *19*, 2244–2259. [CrossRef]

75. Leitner, W. Carbon Dioxide as a Raw Material: The Synthesis of Formic Acid and Its Derivatives from CO$_2$. *Angew. Chem. Int. Ed.* **1995**, *34*, 2207–2221. [CrossRef]

76. Goli, A.; Shamiri, A.; Talaiekhozani, A.; Eshtiaghi, N.; Aghamohammadi, N.; Aroua, M.K. An overview of biological processes and their potential for CO$_2$ capture. *J. Environ. Manag.* **2016**, *183*, 41–58. [CrossRef] [PubMed]

77. Bowyer, J.R.; Leegood, R.C.; Dey, P.M.; Harborne, J.B. *Plant Biochemistry*; Academic Press: Cambridge, MA, USA, 1997.

78. Moseman, A.; Harvey, C. How Many New Trees Would We Need to Offset Our Carbon Emissions? MIT Climate Portal. 2022. Available online: https://climate.mit.edu/ask-mit/how-many-new-trees-would-we-need-offset-our-carbon-emissions (accessed on 29 March 2023).

79. Ramanan, R.; Kannan, K.; Deshkar, A.; Yadav, R.; Chakrabarti, T. Enhanced algal CO$_2$ sequestration through calcite deposition by Chlorella sp. And Spirulina platensis in a mini-raceway pond. *Bioresour. Technol.* **2010**, *101*, 2616–2622. [CrossRef]

80. Surampalli, R.Y.; Zhang, T.C.; Tyagi, R.D.; Naidu, R.; Gurjar, B.R.; Ojha, C.S.P.; Yan, S.; Brar, S.K.; Ramakrishnan, A.; Kao, C.M. (Eds.) *Carbon Capture and Storage: Physical, Chemical, and Biological Methods*; American Society of Civil Engineers: Reston, VA, USA, 2015. [CrossRef]

81. Sayre, R. Microalgae: The Potential for Carbon Capture. *Bioscience* **2010**, *60*, 722–727. [CrossRef]

82. Núñez-López, V.; Moskal, E. Potential of CO$_2$-EOR for Near-Term Decarbonization. *Front. Clim.* **2019**, *1*, 5. [CrossRef]

83. Kuuskraa, V.A.; Godec, M.L.; Dipietro, P. CO$_2$ Utilization from "Next Generation" CO$_2$ Enhanced Oil Recovery Technology. *Energy Procedia* **2013**, *37*, 6854–6866. [CrossRef]

84. Aryana, S.A.; Barclay, C.; Liu, S. North cross Devonian unit-a mature continuous CO$_2$ flood beyond 200% HCPV injection. In Proceedings of the SPE Annual Technical Conference and Exhibition SPE, Amsterdam, The Netherlands, 27–29 October 2014. [CrossRef]

85. Cao, M.; Gu, Y. Physicochemical Characterization of Produced Oils and Gases in Immiscible and Miscible CO$_2$ Flooding Processes. *Energy Fuels* **2012**, *27*, 440–453. [CrossRef]

86. IEA. Number of EOR Projects in Operation Globally, 1971–2017—Charts—Data & Statistics. Available online: https://www.iea.org/data-and-statistics/charts/number-of-eor-projects-in-operation-globally-1971-2017 (accessed on 29 March 2023).

87. Jarrell, P.M.; Fox, C.; Stein, M.; Webb, S. *Practical Aspects of CO$_2$ Flooding*; Society of Petroleum Engineers: Richardson, TX, USA, 2002; Volume 22.

88. International Reservoir Technologies, Inc. IRT EOR Projects. Available online: http://www.irt-inc.com/eor-projects.html (accessed on 29 March 2023).

89. Han, L.; Gu, Y. Optimization of Miscible CO$_2$ Water-Alternating-Gas Injection in the Bakken Formation. *Energy Fuels* **2014**, *28*, 6811–6819. [CrossRef]

90. Jin, L.; Hawthorne, S.; Sorensen, J.; Pekot, L.; Smith, S.; Heebink, L.; Bosshart, N.; Torres, J.; Dalkhaa, C.; Gorecki, C.; et al. Extraction of Oil From the Bakken Shale Formations With Supercritical CO$_2$. In Proceedings of the 5th Unconventional Resources Technology Conference, Austin, TX, USA, 24–26 July 2017. [CrossRef]

91. ENERGY.GOV, Vast Energy Resource in Residual Oil Zones, FE Study Says. Energy.Gov. June 2022. Available online: https://www.energy.gov/fecm/articles/vast-energy-resource-residual-oil-zones-fe-study-says (accessed on 29 March 2023).

92. Honarpour, M.M.; Nagarajan, N.R.; Grijalba, A.C.; Valle, M.; Adesoye, K. Rock-Fluid Characterization for Miscible CO_2 Injection: Residual Oil Zone, Seminole Field, Permian Basin. In Proceedings of the SPE Annual Technical Conference and Exhibition, Florence, Italy, 20–22 September 2010. [CrossRef]

93. Melzer, S. Stranded Oil in The Residual Oil Zone Prepared for Advanced Resources International and U.S. Department of Energy Office of Fossil Energy-Office of Oil and Natural Gas. In *Energy Procedia*; Elsevier: Amsterdam, The Netherlands, 2006. [CrossRef]

94. Burton-Kelly, M.E.; Dotzenrod, N.W.; Feole, I.K.; Peck, W.D.; He, J.; Butler, S.K.; Kurz, M.D.; Kurz, B.A.; Smith, S.A.; Gorecki, C.D. *Identification of Residual Oil Zones in the Williston and Powder River Basins*; DOE-EERC—FE0024453, 1430234; Energy and Environmental Research Center: Grand Forks, ND, USA, 29 March 2018. [CrossRef]

95. Chen, B.; Pawar, R. Capacity Assessment of CO_2 Storage and Enhanced Oil Recovery in Residual Oil Zones. In Proceedings of the SPE Annual Technical Conference and Exhibition, Dallas, TX, USA, 24–26 September 2018. [CrossRef]

96. Roueché, J.N.; Karacan, C.Ö. Zone Identification and Oil Saturation Prediction in a Waterflooded Field: Residual Oil Zone. In Proceedings of the SPE Improved Oil Recovery Conference, Tulsa, OK, USA, 14–18 April 2018. [CrossRef]

97. Ren, B.; Duncan, I. Modeling oil saturation evolution in residual oil zones: Implications for CO_2 EOR and sequestration. *J. Pet. Sci. Eng.* **2019**, *177*, 528–539. [CrossRef]

98. Ren, B.; Duncan, I.J. Reservoir simulation of carbon storage associated with CO_2 EOR in residual oil zones, San Andres formation of West Texas, Permian Basin, USA. *Energy* **2019**, *167*, 391–401. [CrossRef]

99. Puri, R.; Yee, D. Enhanced Coalbed Methane Recovery. In Proceedings of the SPE Annual Technical Conference and Exhibition, New Orleans, Louisiana, 23–26 September 1990. [CrossRef]

100. Moore, T.A. Coalbed methane: A review. *Int. J. Coal Geol.* **2012**, *101*, 36–81. [CrossRef]

101. Flores, R.M. Coalbed methane: From hazard to resource. *Int. J. Coal Geol.* **1998**, *35*, 3–26. [CrossRef]

102. Qin, Y.; Moore, T.A.; Shen, J.; Yang, Z.; Shen, Y.; Wang, G. Resources and geology of coalbed methane in China: A review. *Int. Geol. Rev.* **2017**, *60*, 777–812. [CrossRef]

103. Liang, W.; Yan, J.; Zhang, B.; Hou, D. Review on Coal Bed Methane Recovery Theory and Technology: Recent Progress and Perspectives. *Energy Fuels* **2021**, *35*, 4633–4643. [CrossRef]

104. Mazzotti, M.; Pini, R.; Storti, G. Enhanced coalbed methane recovery. *J. Supercrit. Fluids* **2009**, *47*, 619–627. [CrossRef]

105. Oudinot, A.Y.; Riestenberg, D.E.; Koperna, G.J. Enhanced Gas Recovery and CO_2 Storage in Coal Bed Methane Reservoirs with N_2 Co-Injection. *Energy Procedia* **2017**, *114*, 5356–5376. [CrossRef]

106. Kelemen, P.; Benson, S.M.; Pilorgé, H.; Psarras, P.; Wilcox, J. An Overview of the Status and Challenges of CO_2 Storage in Minerals and Geological Formations. *Front. Clim.* **2019**, *1*, 9. [CrossRef]

107. National Academies of Sciences, Engineering, and Medicine. *Negative Emissions Technologies and Reliable Sequestration: A Research Agenda*; National Academies Press: Washington, DC, USA, 2018. [CrossRef]

108. Global Energy Review: CO_2 Emissions in 2022. 2022. Available online: https://iea.blob.core.windows.net/assets/3c8fa115-35c4-4474-b237-1b00424c8844/CO2Emissionsin2022.pdf (accessed on 29 March 2023).

109. United States National Energy Technology Laboratory; Office of Fossil Energy. *Carbon sequestration ATLAS of the United States and Canada*; National Energy Technology Laboratory: Albany, OR, USA, 2007.

110. Bachu, S. Screening and ranking of sedimentary basins for sequestration of CO_2 in geological media in response to climate change. *Environ. Geol.* **2003**, *44*, 277–289. [CrossRef]

111. Bradshaw, J.; Bachu, S.; Bonijoly, D.; Burruss, R.; Holloway, S.; Christensen, N.P.; Mathiassen, O.M. CO_2 storage capacity estimation: Issues and development of standards. *Int. J. Greenh. Gas Control* **2007**, *1*, 62–68. [CrossRef]

112. Michael, K.; Golab, A.; Shulakova, V.; Ennis-King, J.; Allinson, G.; Sharma, S.K.; Aiken, T. Geological storage of CO_2 in saline aquifers—A review of the experience from existing storage operations. *Int. J. Greenh. Gas Control* **2010**, *4*, 659–667. [CrossRef]

113. Bruant, R.G.; Guswa, A.J.; Celia, M.A.; Peters, C.A. Safe storage of CO_2 in deep saline aquifers. *Environ. Sci. Technol.* **2002**, *36*, 240A–245A. [CrossRef] [PubMed]

114. Jafari, M.; Cao, S.C.; Jung, J. Geological CO_2 sequestration in saline aquifers: Implication on potential solutions of China's power sector. *Resour. Conserv. Recycl.* **2017**, *121*, 137–155. [CrossRef]

115. Hepple, R.P.; Benson, S.M. Geologic storage of carbon dioxide as a climate change mitigation strategy: Performance requirements and the implications of surface seepage. *Environ. Geol.* **2005**, *47*, 576–585. [CrossRef]

116. IEA. *Technology Roadmap: Carbon Capture and Storage*; OECD Publishing: Paris, France, 2009. [CrossRef]

117. Corum, M.D.; Jones, K.B.; Warwick, P.D. CO_2 Sequestration Potential of Unmineable Coal—State of Knowledge. *Energy Procedia* **2013**, *37*, 5134–5140. [CrossRef]

118. Torp, T.A.; Gale, J. Demonstrating storage of CO_2 in geological reservoirs: The Sleipner and SACS projects. *Energy* **2004**, *29*, 1361–1369. [CrossRef]

119. Riddiford, F.; Tourqui, A.; Bishop, C.; Taylor, B.; Smith, M. A Cleaner Development: The in Salah Gas Project, Algeria. In Proceedings of the 6th International Conference on Greenhouse Gas Control Technologies, Kyoto, Japan, 1–4 October 2003; Volume 1, pp. 595–600. [CrossRef]

120. Maldal, T.; Tappel, I.M. CO_2 underground storage for Snøhvit gas field development. *Energy* **2004**, *29*, 1403–1411. [CrossRef]

121. Zhang, L.; Huang, H.; Wang, Y.; Ren, B.; Ren, S.; Chen, G.; Zhang, H. CO_2 storage safety and leakage monitoring in the CCS demonstration project of Jilin oilfield, China. *Greenh. Gases Sci. Technol.* **2014**, *4*, 425–439. [CrossRef]

122. Yang, F.; Bai, B.; Tang, D.; Shari, D.-N.; David, W. Characteristics of CO_2 sequestration in saline aquifers. *Pet. Sci.* **2010**, *7*, 83–92. [CrossRef]

123. Hassanzadeh, H.; Pooladi-Darvish, M.; Keith, D.W. Accelerating CO_2 Dissolution in Saline Aquifers for Geological Storage—Mechanistic and Sensitivity Studies. *Energy Fuels* **2009**, *23*, 3328–3336. [CrossRef]

124. Chadwick, A.; Arts, R.; Bernstone, C.; May, F.; Thibeau, S.; Zweigel, P. (Eds.) *Best Practice for the Storage of CO_2 in Saline Aquifers: Observations and Guidelines from the SACS and CO_2STORE Projects*; British Geological Survey: Nottingham, UK, 2008.

125. De Silva, G.; Ranjith, P.; Perera, M. Geochemical aspects of CO_2 sequestration in deep saline aquifers: A review. *Fuel* **2015**, *155*, 128–143. [CrossRef]

126. Bando, S.; Takemura, F.; Nishio, M.; Hihara, E.; Akai, M. Solubility of CO_2 in Aqueous Solutions of NaCl at (30 to 60) °C and (10 to 20) MPa. *J. Chem. Eng. Data* **2003**, *48*, 576–579. [CrossRef]

127. Portier, S.; Rochelle, C. Modelling CO_2 solubility in pure water and NaCl-type waters from 0 to 300 °C and from 1 to 300 bar: Application to the Utsira Formation at Sleipner. *Chem. Geol.* **2005**, *217*, 187–199. [CrossRef]

128. Pawar, R.J.; Bromhal, G.S.; Carey, J.W.; Foxall, W.; Korre, A.; Ringrose, P.S.; Tucker, O.; Watson, M.N.; White, J.A. Recent advances in risk assessment and risk management of geologic CO_2 storage. *Int. J. Greenh. Gas Control* **2015**, *40*, 292–311. [CrossRef]

129. Gadikota, G.; Matter, J.; Kelemen, P.; Park, A.-H.A. Chemical and morphological changes during olivine carbonation for CO_2 storage in the presence of NaCl and $NaHCO_3$. *Phys. Chem. Chem. Phys.* **2014**, *16*, 4679–4693. [CrossRef] [PubMed]

130. Zendehboudi, S.; Ahmadi, M.A.; Bahadori, A.; Shafiei, A.; Babadagli, T. A developed smart technique to predict minimum miscible pressure-EOR implications. *Can. J. Chem. Eng.* **2013**, *91*, 1325–1337. [CrossRef]

131. Quijada, M.G. Optimization of a CO_2 Flood Design Wasson—West Texas. Master's Thesis, Texas A&M University, Brazos County, TX, USA, 2005. Available online: https://oaktrust.library.tamu.edu/bitstream/handle/1969.1/4138/etd-tamu-2005B-PETE-Garcia.pdf?sequence=1&isAllowed=y (accessed on 29 March 2023).

132. Yellig, W.F.; Metcalfe, R.S. Determination and Prediction of CO_2 Minimum Miscibility Pressures (includes associated paper 8876). *J. Pet. Technol.* **1980**, *32*, 160–168. [CrossRef]

133. Verma, M.K. *Fundamentals of Carbon Dioxide-Enhanced Oil Recovery (CO_2-EOR)—A Supporting Document of the Assessment Methodology for Hydrocarbon Recovery Using CO_2-EOR Associated with Carbon Sequestration*; Open-File Report; US Geological Survey: Washington, DC, USA, 2015.

134. Zhang, N.; Wei, M.; Bai, B. Comprehensive Review of Worldwide CO_2 Immiscible Flooding. In Proceedings of the SPE Improved Oil Recovery Conference, East Seminole Field, TX, USA, 17 April 2018. [CrossRef]

135. Adel, I.A.; Zhang, F.; Bhatnagar, N.; Schechter, D.S. The Impact of Gas-Assisted Gravity Drainage on Operating Pressure in a Miscible CO_2 Flood. In Proceedings of the SPE Improved Oil Recovery Conference, Tulsa, OK, USA, 14–18 April 2018. [CrossRef]

136. Aryana, S.; Kovscek, A.R. Experiments and analysis of drainage displacement processes relevant to carbon dioxide injection. *Phys. Rev. E* **2012**, *86*, 066310. [CrossRef]

137. Zhou, D.; Yan, M.; Calvin Wm, M. Optimization of a Mature CO_2 Flood—From Continuous Injection to WAG. In Proceedings of the SPE Improved Oil Recovery Conference, Tulsa, OK, USA, 14–18 April 2012. [CrossRef]

138. Bellavance, J.F.R. Dollarhide Devonian CO_2 Flood: Project performance review 10 years later. In Proceedings of the Permian Basin Oil and Gas Recovery Conference, Midland, TX, USA, 27–29 March 1996.

139. Wang, X.; Luo, P.; Er, V.; Huang, S. Assessment of CO_2 Flooding Potential for Bakken Formation, Saskatchewan. In Proceedings of the Canadian Unconventional Resources and International Petroleum Conference, Calgary, AB, Canada, 19–21 October 2010. [CrossRef]

140. Ghedan, S. Global Laboratory Experience of CO_2-EOR Flooding. In Proceedings of the SPE/EAGE Reservoir Characterization & Simulation Conference, Abu Dhabi, United Arab Emirates, 19–21 October 2009. [CrossRef]

141. Luis, F.; Al Hammadi, K.; Tanakov, M. Case Study of CO_2 Injection to Enhance Oil Recovery into the Transition Zone of a Tight Carbonate Reservoir. In Proceedings of the Abu Dhabi International Petroleum Exhibition & Conference, Abu Dhabi, United Arab Emirates, 7–10 November 2016. [CrossRef]

142. Parrish, D.R. Flooding Process for Recovery of Oil. U.S. Patent No. 3,244,228, 5 April 1996.

143. Sohrabi, M.; Tehrani, D.H.; Danesh, A.; Henderson, G.D. Visualisation of Oil Recovery by Water Alternating Gas (WAG) Injection Using High Pressure Micromodels—Oil-Wet & Mixed-Wet Systems. In Proceedings of the SPE Annual Technical Conference and Exhibition, New Orleans, Louisiana, 30 September–3 October 2001. [CrossRef]

144. Yoosook, H.; Maneeintr, K. CO_2 geological storage coupled with water alternating gas for enhanced oil recovery. *Chem. Eng. Trans.* **2018**, *63*, 217–222. [CrossRef]

145. Christensen, J.R.; Stenby, E.H.; Skauge, A. Review of WAG field experience. *SPE Reserv. Eval. Eng.* **2001**, *4*, 97–106. [CrossRef]

146. Panjalizadeh, H.; Alizadeh, A.; Ghazanfari, M. Optimization of the WAG Injection Process. *Pet. Sci. Technol.* **2015**, *33*, 294–301. [CrossRef]

147. Kumar, S.; Mandal, A. A comprehensive review on chemically enhanced water alternating gas/CO_2 (CEWAG) injection for enhanced oil recovery. *J. Pet. Sci. Eng.* **2017**, *157*, 696–715. [CrossRef]

148. Kechut, N.I.; Groot, J.A.W.M.; Mustafa, M.A.; Groenenboom, J. Robust Screening Criteria for Foam-Assisted Water-Alternating Gas FAWAG Injection. In Proceedings of the SPE/IATMI Asia Pacific Oil & Gas Conference and Exhibition, Virtual, 10–12 October 2021. [CrossRef]

149. Omar, S.; Jaafar, M.Z.; Ismail, A.R.; Sulaiman, W.R. Monitoring Foam Stability in Foam Assisted Water Alternate Gas (FAWAG) Processes Using Electrokinetic Signals. In Proceedings of the SPE Enhanced Oil Recovery Conference, Kuala Lumpur, Malaysia, 2–4 July 2013. [CrossRef]

150. Tetteh, J.T.; Cudjoe, S.E.; Aryana, S.A.; Ghahfarokhi, R.B. Investigation into fluid-fluid interaction phenomena during low salinity waterflooding using a reservoir-on-a-chip microfluidic model. *J. Pet. Sci. Eng.* **2021**, *196*, 108074. [CrossRef]

151. Khan, M.Y.; Kohata, A.; Patel, H.; Syed, F.I.; Al Sowaidi, A.K. Water Alternating Gas WAG Optimization Using Tapered WAG Technique for a Giant Offshore Middle East Oil Field. In Proceedings of the Abu Dhabi International Petroleum Exhibition & Conference, Abu Dhabi, United Arab Emirates, 7–10 November 2016. [CrossRef]

152. Kohata, A.; Willingham, T.; Yunus Khan, M.; Al Sowaidi, A. Extensive Miscible Water Alternating Gas WAG Simulation Study for a Giant Offshore Oil Field. In Proceedings of the Abu Dhabi International Petroleum Exhibition & Conference, Abu Dhabi, United Arab Emirates, 13–16 November 2017. [CrossRef]

153. Wang, Y.; Mckinzie, J.; Furtado, F.; Aryana, S.A. Scaling Analysis of Two-Phase Flow in Fractal Permeability Fields. *Water Resour. Res.* **2020**, *56*, e2020WR028214. [CrossRef]

154. Guo, F.; Aryana, S. An experimental investigation of nanoparticle-stabilized CO_2 foam used in enhanced oil recovery. *Fuel* **2016**, *186*, 430–442. [CrossRef]

155. Heller, J.P.; Lien, C.L.; Kuntamukkula, M.S. Foamlike Dispersions for Mobility Control in CO_2 Floods. *Soc. Pet. Eng. J.* **1985**, *25*, 603–613. [CrossRef]

156. Hosseini, H.; Tsau, J.S.; Wasserbauer, J.; Aryana, S.A.; Ghahfarokhi, R.B. Synergistic foam stabilization and transport improvement in simulated fractures with polyelectrolyte complex nanoparticles: Microscale observation using laser etched glass micromodels. *Fuel* **2021**, *301*, 121004. [CrossRef]

157. Bond, D.C.; Holbrook, O.C. Gas Dreve Ol Recovery Process (United States Patent Office Patent No. 630087). 1956. Available online: https://patentimages.storage.googleapis.com/30/d4/db/dc81eb4f3af9db/US2866507.pdf (accessed on 29 March 2023).

158. Afzali, S.; Rezaei, N.; Zendehboudi, S. A comprehensive review on Enhanced Oil Recovery by Water Alternating Gas (WAG) injection. *Fuel* **2018**, *227*, 218–246. [CrossRef]

159. Sheng, J.J. Foams and Their Applications in Enhancing Oil Recovery. In *Enhanced Oil Recovery Field Case Studies*; Elsevier: Amsterdam, The Netherlands, 2013; pp. 251–280. [CrossRef]

160. Qingfeng, H.; Zhu, Y.; Luo, Y.; Weng, R. Studies On Foam Flooding EOR Technique For Daqing Reservoirs After Polymer Flooding. In Proceedings of the SPE Improved Oil Recovery Symposium, Tulsa, OK, USA, 14–18 April 2012. [CrossRef]

161. Guo, F.; Aryana, S.A. Improved sweep efficiency due to foam flooding in a heterogeneous microfluidic device. *J. Pet. Sci. Eng.* **2018**, *164*, 155–163. [CrossRef]

162. Guo, F.; Aryana, S.A. Foam Flooding in a Heterogeneous Porous Medium. In *Advances in Petroleum Engineering and Petroleum Geochemistry*; Banerjee, S., Barati, R., Patil, S., Eds.; Springer International Publishing: Berlin/Heidelberg, Germany, 2019; pp. 65–67. [CrossRef]

163. Sunmonu, R.M.; Onyekonwu, M. Enhanced Oil Recovery using Foam Injection; a Mechanistic Approach. In Proceedings of the SPE Nigeria Annual International Conference and Exhibition, Lagos, Nigeria, 5–7 August 2013. [CrossRef]

164. Ma, K.; Lopez-Salinas, J.L.; Puerto, M.C.; Miller, C.A.; Biswal, S.L.; Hirasaki, G.J. Estimation of Parameters for the Simulation of Foam Flow through Porous Media. Part 1: The Dry-Out Effect. *Energy Fuels* **2013**, *27*, 2363–2375. [CrossRef]

165. Lake, L.W. *Enhanced Oil Recovery*; Prentice Hall: Englewood Cliffs, NJ, USA, 1989.

166. Belyadi, H.; Fathi, E.; Belyadi, F. Hydraulic fracturing fluid systems. In *Hydraulic Fracturing in Unconventional Reservoirs*; Elsevier: Amsterdam, The Netherlands, 2019; pp. 47–69. [CrossRef]

167. David, A.; Marsden, S.S. The Rheology of Foam. In Proceedings of the Fall Meeting of the Society of Petroleum Engineers of AIME, Denver, Colorado, 28 September–1 October 1969.

168. Emadi, S.; Shadizadeh, S.R.; Manshad, A.K.; Rahimi, A.M.; Nowrouzi, I.; Mohammadi, A.H. Effect of using Zyziphus Spina Christi or Cedr Extract (CE) as a natural surfactant on oil mobility control by foam flooding. *J. Mol. Liq.* **2019**, *293*, 111573. [CrossRef]

169. Ma, K.; Liontas, R.; Conn, C.A.; Hirasaki, G.J.; Biswal, S.L. Visualization of improved sweep with foam in heterogeneous porous media using microfluidics. *Soft Matter* **2012**, *8*, 10669–10675. [CrossRef]

170. AlQuaimi, B.I.; Rossen, W.R. Foam Generation and Rheology in a Variety of Model Fractures. *Energy Fuels* **2019**, *33*, 68–80. [CrossRef]

171. Gajbhiye, R. Novel CO_2/N2 Foam Concept and Optimization Scheme for Improving CO_2-foam EOR Process. In Proceedings of the SPE Middle East Oil & Gas Show and Conference, event canceled, 28 November–1 December 2021. [CrossRef]

172. Chang, S.-H.; Grigg, R.B. Effects of Foam Quality and Flow Rate on CO_2-Foam Behavior at Reservoir Temperature and Pressure. *SPE Reserv. Eval. Eng.* **1999**, *2*, 248–254. [CrossRef]

173. Patton, J.T.; Holbrook, S.T.; Hsu, W. Rheology of Mobility-Control Foams. *Soc. Pet. Eng. J.* **1983**, *23*, 456–460. [CrossRef]

174. Khatib, Z.I.; Hirasaki, G.J.; Falls, A.H. Effects of Capillary Pressure on Coalescence and Phase Mobilities in Foams Flowing Through Porous Media. *SPE Reserv. Eng.* **1988**, *3*, 919–926. [CrossRef]

175. Mirzaei, M.; Kumar, D.; Turner, D.; Shock, A.; Andel, D.; Hampton, D.; Knight, T.E.; Katiyar, A.; Patil, P.D.; Rozowski, P.; et al. CO_2 Foam Pilot in a West Texas Field: Design, Operation and Results. In Proceedings of the SPE Improved Oil Recovery Conference, Virtual, 31 August–4 September 2020. [CrossRef]

176. Føyen, T.; Brattekås, B.; Fernø, M.; Barrabino, A.; Holt, T. Increased CO_2 storage capacity using CO_2-foam. *Int. J. Greenh. Gas Control* **2020**, *96*, 103016. [CrossRef]

177. Sheng, J.; Maini, B.; Hayes, R.; Tortike, W. Experimental Study of Foamy Oil Stability. *J. Can. Pet. Technol.* **1997**, *36*, 31–37. [CrossRef]

178. Yu, W.; Kanj, M.Y. Review of foam stability in porous media: The effect of coarsening. *J. Pet. Sci. Eng.* **2022**, *208*, 109698. [CrossRef]

179. Suffridge, F.E.; Raterman, K.T.; Russell, G.C. Foam Performance Under Reservoir Conditions. In Proceedings of the SPE Annual Technical Conference and Exhibition, San Antonio, TX, USA, 8–11 October 1989. [CrossRef]

180. Louvet, N.; Rouyer, F.; Pitois, O. Ripening of a draining foam bubble. *J. Colloid Interface Sci.* **2009**, *334*, 82–86. [CrossRef]

181. Saint-Jalmes, A. Physical chemistry in foam drainage and coarsening. *Soft Matter* **2006**, *2*, 836–849. [CrossRef]

182. Fan, C.; Jia, J.; Peng, B.; Liang, Y.; Li, J.; Liu, S. Molecular Dynamics Study on CO_2 Foam Films with Sodium Dodecyl Sulfate: Effects of Surfactant Concentration, Temperature, and Pressure on the Interfacial Tension. *Energy Fuels* **2020**, *34*, 8562–8574. [CrossRef]

183. Guo, F.; He, J.; Johnson, P.A.; Aryana, S.A. Stabilization of CO_2foam using by-product fly ash and recyclable iron oxide nanoparticles to improve carbon utilization in EOR processes. *Sustain. Energy Fuels* **2017**, *1*, 814–822. [CrossRef]

184. Yu, J.; An, C.; Mo, D.; Liu, N.; Lee, R. Foam Mobility Control for Nanoparticle-Stabilized CO_2 Foam. In Proceedings of the SPE Improved Oil Recovery Symposium, Tulsa, OK, USA, 14–18 April 2012. [CrossRef]

185. Nazari, N.; Tsau, J.-S.; Barati, R. CO_2 Foam Stability Improvement Using Polyelectrolyte Complex Nanoparticles Prepared in Produced Water. *Energies* **2017**, *10*, 516. [CrossRef]

186. Binks, B.P. Particles as surfactants similarities and differences. *Interface Sci.* **2002**, *7*, 21–41.

187. Binks, B.P.; Horozov, T.S. Aqueous Foams Stabilized Solely by Silica Nanoparticles. *Angew. Chem. Int. Ed.* **2005**, *44*, 3722–3725. [CrossRef]

188. Fu, C.; Liu, N. Rheology and stability of nanoparticle-stabilized CO_2 foam under reservoir conditions. *J. Pet. Sci. Eng.* **2021**, *196*, 107671. [CrossRef]

189. Rognmo, A.; Heldal, S.; Fernø, M. Silica nanoparticles to stabilize CO_2-foam for improved CO_2 utilization: Enhanced CO_2 storage and oil recovery from mature oil reservoirs. *Fuel* **2018**, *216*, 621–626. [CrossRef]

190. Alargova, R.G.; Warhadpande, D.S.; Paunov, V.N.; Velev, O.D. Foam Superstabilization by Polymer Microrods. *Langmuir* **2004**, *20*, 10371–10374. [CrossRef]

191. Guo, F.; Aryana, S.A. Nanoparticle-Stabilized CO_2 Foam Flooding. In *Advances in Petroleum Engineering and Petroleum Geochemistry*; Banerjee, S., Barati, R., Patil, S., Eds.; Springer International Publishing: Berlin/Heidelberg, Germany, 2019; pp. 61–63. [CrossRef]

192. Worthen, A.J.; Parikh, P.S.; Chen, Y.; Bryant, S.L.; Huh, C.; Johnston, K.P. Carbon Dioxide-in-Water Foams Stabilized with a Mixture of Nanoparticles and Surfactant for CO_2 Storage and Utilization Applications. *Energy Procedia* **2014**, *63*, 7929–7938. [CrossRef]

193. Worthen, A.J.; Bryant, S.L.; Huh, C.; Johnston, K.P. Carbon dioxide-in-water foams stabilized with nanoparticles and surfactant acting in synergy. *AIChE J.* **2013**, *59*, 3490–3501. [CrossRef]

194. Agista, M.N.; Guo, K.; Yu, Z. A state-of-the-art review of nanoparticles application in petroleum with a focus on enhanced oil recovery. *Appl. Sci.* **2018**, *8*, 871. [CrossRef]

195. Liu, Q.; Qu, H.; Liu, S.; Zhang, Y.; Zhang, S.; Liu, J.; Peng, B.; Luo, D. Modified Fe_3O_4 nanoparticle used for stabilizing foam flooding for enhanced oil recovery. *Colloids Surf. A Physicochem. Eng. Asp.* **2020**, *605*, 125383. [CrossRef]

196. Liu, Q.; Zhang, Y.; Zhao, X.; Ye, H.; Luo, D. Enhanced oil recovery by foam flooding using foam stabilized with modified Fe_3O_4 nanoparticles. *J. Pet. Sci. Eng.* **2022**, *209*, 109850. [CrossRef]

197. Nazari, N.; Hosseini, H.; Tsau, J.S.; Shafer-Peltier, K.; Marshall, C.; Ye, Q.; Ghahfarokhi, R.B. Development of highly stable lamella using polyelectrolyte complex nanoparticles: An environmentally friendly scCO2 foam injection method for CO_2 utilization using EOR. *Fuel* **2020**, *261*, 116360. [CrossRef]

198. Bhatt, S.; Saraf, S.; Bera, A. Perspectives of Foam Generation Techniques and Future Directions of Nanoparticle-Stabilized CO_2 Foam for Enhanced Oil Recovery. *Energy Fuels* **2023**, *37*, 1472–1494. [CrossRef]

199. Rossen, W.R. A critical review of Roof snap-off as a mechanism of steady-state foam generation in homogeneous porous media. *Colloids Surf. A Physicochem. Eng. Asp.* **2003**, *225*, 1–24. [CrossRef]

200. Ransohoff, T.C.; Radke, C.J. Mechanisms of Foam Generation in Glass-Bead Packs. *SPE Reserv. Eng.* **1988**, *3*, 573–585. [CrossRef]

201. Gauteplass, J.; Chaudhary, K.; Kovscek, A.R.; Fernø, M.A. Pore-level foam generation and flow for mobility control in fractured systems. *Colloids Surf. A Physicochem. Eng. Asp.* **2015**, *468*, 184–192. [CrossRef]

202. Wu, Y.; Fang, S.; Dai, C.; Sun, Y.; Fang, J.; Liu, Y.; He, L. Investigation on bubble snap-off in 3-D pore-throat micro-structures. *J. Ind. Eng. Chem.* **2017**, *54*, 69–74. [CrossRef]

203. Hosseini, H.; Guo, F.; Ghahfarokhi, R.B.; Aryana, S.A. Microfluidic Fabrication Techniques for High-Pressure Testing of Microscale Supercritical CO_2 Foam Transport in Fractured Unconventional Reservoirs. *J. Vis. Exp.* **2020**, *161*, 61369. [CrossRef]

204. Holloway, S. (Ed.) *The Underground Disposal of Carbon Dioxide*; British Geological Survey: Nottingham, UK, 1996.

205. Damen, K.; Faaij, A.; Turkenburg, W. Health, Safety and Environmental Risks of Underground CO₂ Storage—Overview of Mechanisms and Current Knowledge. *Clim. Chang.* **2006**, *74*, 289–318. [CrossRef]
206. He, M.; Luis, S.; Rita, S.; Ana, G.; Euripedes, V.; Zhang, N. Risk assessment of CO₂ injection processes and storage in carboniferous formations: A review. *J. Rock Mech. Geotech. Eng.* **2011**, *3*, 39–56. [CrossRef]
207. Piessens, K.; Dusar, M. *CO₂-Sequestration in Abandoned Coal Mines*; Royal Belgian Institute for Natural Sciences: Brussels, Belgium, 2003. Available online: https://www.naturalsciences.be/sites/default/files/sequestration.pdf (accessed on 29 March 2023).
208. Price, P.N.; McKone, T.E.; Sohn, M.D. *Carbon Sequestration Risks and Risk Management*; Lawrence Berkeley National Laboratory: Berkeley, CA, USA, 2008. Available online: https://escholarship.org/uc/item/0x18n8qm (accessed on 29 March 2023).
209. Solomon, S. Carbon Dioxide Storage: Geological Security and Environmental Issues—Case Study on the Sleipner Gas Field in Norway. Bellona report. 2006. Available online: https://bellona.no/content/uploads/Carbon-Dioxide-Storage.pdf (accessed on 29 March 2023).
210. Jarup, L. Hazards of heavy metal contamination. *Br. Med. Bull.* **2003**, *68*, 167–182. [CrossRef] [PubMed]
211. Siirila, E.R.; Navarre-Sitchler, A.K.; Maxwell, R.M.; McCray, J.E. A quantitative methodology to assess the risks to human health from CO₂ leakage into groundwater. *Adv. Water Resour.* **2012**, *36*, 146–164. [CrossRef]
212. Do, H.-K.; Yun, S.-T.; Yu, S.; Ryuh, Y.-G.; Choi, H.-S. Evaluation of long-term impacts of CO₂ leakage on groundwater quality using hydrochemical data from a natural analogue site in South Korea. *Water* **2020**, *12*, 1457. [CrossRef]
213. Mortezaei, K.; Vahedifard, F. Numerical Simulation of Induced Seismicity in Carbon Capture and Storage Projects. *Geotech. Geol. Eng.* **2015**, *33*, 411–424. [CrossRef]
214. Zoback, M.D.; Harjes, H.-P. Injection-induced earthquakes and crustal stress at 9 km depth at the KTB deep drilling site, Germany. *J. Geophys. Res. Solid Earth* **1997**, *102*, 18477–18491. [CrossRef]
215. Rutqvist, J. The Geomechanics of CO₂ Storage in Deep Sedimentary Formations. *Geotech. Geol. Eng.* **2012**, *30*, 525–551. [CrossRef]
216. Mathieson, A.; Midgley, J.; Dodds, K.; Wright, I.; Ringrose, P.; Saoul, N. CO₂ sequestration monitoring and verification technologies applied at Krechba, Algeria. *Geophysics* **2010**, *29*, 216–222. [CrossRef]
217. Teatini, P.; Gambolati, G.; Ferronato, M.; Settari, A.; Walters, D. Land uplift due to subsurface fluid injection. *J. Geodyn.* **2011**, *51*, 1–16. [CrossRef]
218. Healy, J.H.; Rubey, W.W.; Griggs, D.T.; Raleigh, C.B. The Denver Earthquakes. *Science* **1968**, *161*, 1301–1310. [CrossRef] [PubMed]
219. Abanades, J.C.; Akai, M.; Benson, S.; Leone, S.; Doctor, R.; Gale, J.; Keith, D.; Mazzotti, M.; Metz, B.; Meyer, L.; et al. IPCC Special Report—Carbon Dioxide Capture and Storage. 2005. Available online: https://www.ipcc.ch/site/assets/uploads/2018/03/srccs_summaryforpolicymakers-1.pdf (accessed on 29 March 2023).
220. Bickle, M.J. Geological carbon storage. *Nat. Geosci.* **2009**, *2*, 815–818. [CrossRef]
221. Vilarrasa, V.; Olivella, S.; Carrera, J.; Rutqvist, J. Long term impacts of cold CO₂ injection on the caprock integrity. *Int. J. Greenh. Gas Control* **2014**, *24*, 1–13. [CrossRef]
222. Gaus, I. Role and impact of CO₂–rock interactions during CO₂ storage in sedimentary rocks. *Int. J. Greenh. Gas Control* **2010**, *4*, 73–89. [CrossRef]
223. Busch, A.; Amann, A.; Bertier, P.; Waschbusch, M.; Krooss, B.M. The Significance of Caprock Sealing Integrity for CO₂ Storage. In Proceedings of the SPE International Conference on CO₂ Capture, Storage, and Utilization, New Orleans, LA, USA, 10–12 November 2010. [CrossRef]
224. Carroll, S.; Carey, J.W.; Dzombak, D.; Huerta, N.J.; Li, L.; Richard, T.; Um, W.; Walsh, S.D.; Zhang, L. Review: Role of chemistry, mechanics, and transport on well integrity in CO₂ storage environments. *Int. J. Greenh. Gas Control* **2016**, *49*, 149–160. [CrossRef]
225. Anderson, S.T. Risk, Liability, and Economic Issues with Long-Term CO₂ Storage—A Review. *Nat. Resour. Res.* **2017**, *26*, 89–112. [CrossRef]
226. McElmo Dome. 2021. Available online: https://www.gem.wiki/McElmo_Dome (accessed on 29 March 2023).
227. Varanasi, A. You Asked: Does Carbon Capture Technology Actually Work? 27 September 2019. Available online: https://news.climate.columbia.edu/2019/09/27/carbon-capture-technology/#:~:text=The%20first%20carbon%20capture%20plant,Sleipner%2C%20in%20the%20North%20Sea (accessed on 29 March 2023).
228. US EPA. History of the UIC Program—Injection Well Time Line. 4 May 2012. Available online: https://web-ded.uta.edu/cedwebfiles/eti/OP_Fact_Sheet/Underground_Injection_Control/UIC%20History.pdf (accessed on 29 March 2023).
229. US EPA. Federal Requirements Under the Underground Injection Control (UIC) Program for Carbon Dioxide (CO₂) Geologic Sequestration (GS) Wells; Final Rule. *Fed. Regist.* **2010**, *75*. Available online: https://www.govinfo.gov/content/pkg/FR-2010-12-10/pdf/2010-29954.pdf (accessed on 29 March 2023).
230. DOE. Carbon Storage Research. Energy.Gov. 2022. Available online: https://www.energy.gov/fecm/science-innovation/carbon-capture-and-storage-research (accessed on 29 March 2023).
231. UNFCCC. What is the Kyoto Protocol? | UNFCCC. 2022. Available online: https://unfccc.int/kyoto_protocol (accessed on 29 March 2023).
232. Global CCS Institute. CCS: A Solution to Climate Change Right Beneath Our Feet. 2018. Available online: https://unfccc.int/sites/default/files/resource/40_UNFCCC%20Submission_Global%20CCS%20Institute.pdf (accessed on 29 March 2023).
233. Dwortzan, M. This Is How Carbon Capture Could Help Us Meet Key Paris Agreement Goals. World Economic Form. 2 August 2021. Available online: https://www.weforum.org/agenda/2021/08/this-is-how-carbon-capture-could-help-us-meet-key-paris-agreement-goals (accessed on 29 March 2023).

234. UNFCCC. Carbon Capture, Use and Storage. United Nations Framework Convention on Climate Change. 2014. Available online: https://unfccc.int/resource/climateaction2020/tep/thematic-areas/carbon-capture/index.html (accessed on 29 March 2023).

235. HSBC. Carbon Capture & Storage. HSBC. 3 November 2020. Available online: https://www.sustainablefinance.hsbc.com/carbon-transition/carbon-capture-and-storage (accessed on 29 March 2023).

236. Bazilian, M.; Coddington, K. Carbon Capture, Utilization, and Storage Under the Paris Agreement. The Hill. 15 April 2020. Available online: https://thehill.com/opinion/energy-environment/492990-carbon-capture-utilization-and-storage-under-the-paris-agreement/ (accessed on 29 March 2023).

237. Internal Revenue Code. Title 26. 2022. Available online: https://www.govinfo.gov/content/pkg/USCODE-2021-title26/pdf/USCODE-2021-title26-subtitleA-chap1-subchapA-partIV-subpartD-sec45Q.pdf (accessed on 29 March 2023).

238. Orr, F.M.J. Carbon Capture, Utilization, and Storage: An Update. *SPE J.* **2018**, *23*, 2444–2455. [CrossRef]

239. Pollak, M.; Phillips, S.J.; Vajjhala, S. Carbon capture and storage policy in the United States: A new coalition endeavors to change existing policy. *Glob. Environ. Chang.* **2011**, *21*, 313–323. [CrossRef]

240. Carbon Capture Coalition. Federal Policy Blueprint. 2021. Available online: https://carboncapturecoalition.org/wp-content/uploads/2021/02/2021_Blueprint.pdf (accessed on 29 March 2023).

241. US EPA. Underground Injection Control Well Classes [Overviews and Factsheets]. 11 June 2015. Available online: https://www.epa.gov/uic/underground-injection-control-well-classes (accessed on 29 March 2023).

242. US EPA. Primary Enforcement Authority for the Underground Injection Control Program [Overviews and Factsheets]. 22 May 2015. Available online: https://www.epa.gov/uic/primary-enforcement-authority-underground-injection-control-program (accessed on 29 March 2023).

243. EASAC. Carbon Capture and Storage in Europe. 2013. Available online: https://easac.eu/fileadmin/Reports/Easac_13_CCS_Web_Complete.pdf (accessed on 29 March 2023).

244. UNEP. *Basel Convention*; United Nations Environment Programme (UNEP): Nairobi, Kenya, 2020.

245. OSPAR. OSPAR Convention. 2007. Available online: https://www.ospar.org/convention/text (accessed on 29 March 2023).

246. IMO. Convention on the Prevention of Marine Pollution by Dumping of Wastes and Other Matter. International Marine Organisation. 2006. Available online: https://www.imo.org/en/OurWork/Environment/Pages/London-Convention-Protocol.aspx (accessed on 29 March 2023).

247. European Commission. Implementation of Directive 2009/31/EC on the Geological Storage of Carbon Dioxide: Guidance Document 2, Characterisation of the Storage Complex, CO_2 Stream Composition, Monitoring and Corrective Measures. Publications Office. 2011. Available online: https://data.europa.eu/doi/10.2834/98293 (accessed on 29 March 2023).

248. Arts, R.; Winthaegen, P. Monitoring Options for CO_2 Storage. In *Carbon Dioxide Capture for Storage in Deep Geologic Formations*; Elsevier: Amsterdam, The Netherlands, 2005; pp. 1001–1013. [CrossRef]

249. Kikani, J. *Reservoir Surveillance*; Society Of Petroleum Engineers: Richardson, TX, USA, 2013. [CrossRef]

250. DOE/NETL. BEST PRACTICES: Monitoring, Verification, and Accounting (MVA) for Geologic Storage Projects. 2017. Available online: https://netl.doe.gov/sites/default/files/2018-10/BPM-MVA-2012.pdf (accessed on 29 March 2023).

251. DOE/NETL. Permanence and Safety of CCS. Netl.Doe.Gov. 2022. Available online: https://netl.doe.gov/coal/carbon-storage/faqs/permanence-safety (accessed on 29 March 2023).

252. Benson, S.M.; Myer, L.R.; Oldenburg, C.M.; Doughty, C.A.; Pruess, K.; Lewicki, J.; Hoversten, M.; Gasperikova, E.; Daley, T.; Majer, E.; et al. *GEO-SEQ Best Practices Manual. Geologic Carbon Dioxide Sequestration: Site Evaluation to Implementation*; LBNL—56623; Lawrence Berkeley National Laboratory (LBNL): Berkeley, CA, USA, 2004; p. 842996. [CrossRef]

253. Plasynski, S.I.; Litynski, J.T.; McIlvried, H.G.; Vikara, D.M.; Srivastava, R.D. The critical role of monitoring, verification, and accounting for geologic carbon dioxide storage projects. *Environ. Geosci.* **2011**, *18*, 19–34. [CrossRef]

254. EPA. Subpart RR—Geologic Sequestration of Carbon Dioxide. 2023. Available online: https://www.epa.gov/ghgreporting/subpart-rr-geologic-sequestration-carbon-dioxide (accessed on 29 March 2023).

255. California Air Resources Board, 2018, Carbon Capture and Sequestration Protocol under the Low Carbon Fuel Standard. 13 August 2018. Available online: https://ww2.arb.ca.gov/sites/default/files/2020-03/CCS_Protocol_Under_LCFS_8-13-18_ada.pdf (accessed on 29 March 2023).

256. Chadwick, R.A.; Marchant, B.P.; Williams, G.A. CO_2 storage monitoring: Leakage detection and measurement in subsurface volumes from 3D seismic data at Sleipner. *Energy Procedia* **2014**, *63*, 4224–4239. [CrossRef]

257. Pak, N.M.; Rempillo, O.; Norman, A.-L.; Layzell, D.B. Early atmospheric detection of carbon dioxide from carbon capture and storage sites. *J. Air Waste Manag. Assoc.* **2016**, *66*, 739–747. [CrossRef]

258. Cámara, C.; Pérez-Conde, C.; Moreno-Bondi, M.C.; Rivas, C. Fiber optical sensors applied to field measurements. In *Techniques and Instrumentation in Analytical Chemistry*; Elsevier: Amsterdam, The Netherlands, 1995; Volume 17, pp. 165–193. [CrossRef]

259. Park, J.; Cho, H.; Yi, S. NDIR CO_2 gas sensor with improved temperature compensation. *Procedia Eng.* **2010**, *5*, 303–306. [CrossRef]

260. McNeal, M.P.; Moelders, N.; Pralle, M.U.; Puscasu, I.; Last, L.; Ho, W.; Greenwald, A.C.; Daly, J.T.; Johnson, E.A.; George, T. Development of Optical MEMS CO_2 Sensors. In Proceedings of the SPIE Atmospheric Radiation Measurements and Applications in Climate, Seattle, WA, USA, 5 September 2002; Volume 4815, pp. 30–35. [CrossRef]

261. Charpentier, F.; Bureau, B.; Troles, J.; Boussard-Plédel, C.; Pierrès, K.M.-L.; Smektala, F.; Adam, J.-L. Infrared monitoring of underground CO_2 storage using chalcogenide glass fibers. *Opt. Mater.* **2009**, *31*, 496–500. [CrossRef]

262. Jones, D.; Barlow, T.; Beaubien, S.; Ciotoli, G.; Lister, T.; Lombardi, S.; May, F.; Möller, I.; Pearce, J.; Shaw, R. New and established techniques for surface gas monitoring at onshore CO_2 storage sites. *Energy Procedia* **2009**, *1*, 2127–2134. [CrossRef]

263. Leuning, R.; Etheridge, D.; Luhar, A.; Dunse, B. Atmospheric monitoring and verification technologies for CO_2 geosequestration. *Int. J. Greenh. Gas Control* **2008**, *2*, 401–414. [CrossRef]

264. Etheridge, D.; Leuning, R.; Luhar, A.; Spencer, D.; Coram, S.; Steele, L.P.; Zegelin, S.; Allison, C.; Fraser, P.; Porter, L.; et al. Atmospheric monitoring and verification of geosequestration at the CO_2CRC Otway Project. 2007. Available online: http://www.cmar.csiro.au/e-print/open/2007/etheridgedm_a.pdf (accessed on 29 March 2023).

265. Etheridge, D.; Luhar, A.; Loh, Z.; Leuning, R.; Spencer, D.; Steele, P.; Zegelin, S.; Allison, C.; Krummel, P.; Leist, M.; et al. Atmospheric monitoring of the CO_2CRC Otway Project and lessons for large scale CO_2 storage projects. *Energy Procedia* **2011**, *4*, 3666–3675. [CrossRef]

266. Aubinet, M.; Vesala, T.; Papale, D. (Eds.) *Eddy Covariance: A Practical Guide to Measurement and Data Analysis*; Springer: Dordrecht, The Netherlands, 2012. [CrossRef]

267. Rixen, T.; Wit, F.; Hutahaean, H.; Schlüter, A.; Baum, A.; Klemme, A.; Müller, M.; Pranowo, W.S.; Samiaji, J.; Warneke, T. Carbon cycle in tropical peatlands and coastal seas. In *Science for the Protection of Indonesian Coastal Ecosystems (SPICE)*; Elsevier: Amsterdam, The Netherlands, 2022. [CrossRef]

268. Massman, W.; Lee, X. Eddy covariance flux corrections and uncertainties in long-term studies of carbon and energy exchanges. *Agric. For. Meteorol.* **2002**, *113*, 121–144. [CrossRef]

269. Leuning, R.; King, K.M. Comparison of eddy-covariance measurements of CO_2 fluxes by open- and closed-path CO_2 analysers. *Bound. Layer Meteorol.* **1992**, *59*, 297–311. [CrossRef]

270. Suyker, A.E.; Verma, S.B. Eddy correlation measurement of CO_2 flux using a closed-path sensor: Theory and field tests against an open-path sensor. *Bound. Layer Meteorol.* **1993**, *64*, 391–407. [CrossRef]

271. Lewicki, J.L.; Hilley, G.E.; Fischer, M.L.; Pana, L.; Oldenburg, C.M.; Dobeck, L.; Spangler, L. Detection of CO_2 leakage by eddy covariance during the ZERT project's CO_2 release experiments. *Energy Procedia* **2009**, *1*, 2301–2306. [CrossRef]

272. Whittaker, S.; Rostron, B.; Hawkes, C.; Gardner, C.; White, D.; Johnson, J.; Chalaturnyk, R.; Seeburger, D. A decade of CO_2 injection into depleting oil fields: Monitoring and research activities of the IEA GHG Weyburn-Midale CO_2 Monitoring and Storage Project. *Energy Procedia* **2011**, *4*, 6069–6076. [CrossRef]

273. Emberley, S.; Hutcheon, I.; Shevalier, M.; Durocher, K.; Gunter, W.; Perkins, E. Geochemical monitoring of fluid-rock interaction and CO_2 storage at the Weyburn CO_2-injection enhanced oil recovery site, Saskatchewan, Canada. *Energy* **2004**, *29*, 1393–1401. [CrossRef]

274. Sayegh, S.G.; Krause, F.F.; Girard, M.; DeBree, C. Rock/Fluid Interactions of Carbonated Brines in a Sandstone Reservoir: Pembina Cardium, Alberta, Canada. *SPE Form. Eval.* **1990**, *5*, 399–405. [CrossRef]

275. May, F.; Waldmann, S. Tasks and challenges of geochemical monitoring. *Greenh. Gases Sci. Technol.* **2014**, *4*, 176–190. [CrossRef]

276. Freifeld, B.M.; Trautz, R.C. Real-time quadrupole mass spectrometer analysis of gas in borehole fluid samples acquired using the U-tube sampling methodology. *Geofluids* **2006**, *6*, 217–224. [CrossRef]

277. Zimmer, M.; Erzinger, J.; Kujawa, C. The gas membrane sensor (GMS): A new method for gas measurements in deep boreholes applied at the CO_2SINK site. *Int. J. Greenh. Gas Control* **2011**, *5*, 995–1001. [CrossRef]

278. McColpin, G.R. Surface Deformation Monitoring As a Cost Effective MMV Method. *Energy Procedia* **2009**, *1*, 2079–2086. [CrossRef]

279. Du, J.; Brissenden, S.J.; McGillivray, P.; Bourne, S.; Hofstra, P.; Davis, E.J.; Roadarmel, W.H.; Wolhart, S.L.; Wright, C.A. Mapping Fluid Flow in a Reservoir Using Tiltmeter-Based Surface-Deformation Measurements. In Proceedings of the SPE Annual Technical Conference and Exhibition, Dallas, TX, USA, 9–12 October 2005. [CrossRef]

280. Harbert, W.; Daley, T.M.; Bromhal, G.; Sullivan, C.; Huang, L. Progress in monitoring strategies for risk reduction in geologic CO_2 storage. *Int. J. Greenh. Gas Control* **2016**, *51*, 260–275. [CrossRef]

281. Hu, B.; Li, H.; Zhang, X.; Fang, L. Oil and Gas Mining Deformation Monitoring and Assessments of Disaster: Using Interferometric Synthetic Aperture Radar Technology. *IEEE Geosci. Remote Sens. Mag.* **2020**, *8*, 108–134. [CrossRef]

282. Vasco, D.W.; Dixon, T.H.; Ferretti, A.; Samsonov, S.V. Monitoring the fate of injected CO_2 using geodetic techniques. *Geophysics* **2020**, *39*, 29–37. [CrossRef]

283. Vasco, D.W.; Rucci, A.; Ferretti, A.; Novali, F.; Bissell, R.C.; Ringrose, P.S.; Mathieson, A.S.; Wright, I.W. Satellite-Based Measurements of Surface Deformation Reveal Fluid Flow Associated with the Geological Storage of Carbon Dioxide. *Geophys. Res. Lett.* **2010**, 37. [CrossRef]

284. US EPA. Class VI—Wells used for Geologic Sequestration of Carbon Dioxide. 12 September 2022. Available online: https://www.epa.gov/uic/class-vi-wells-used-geologic-sequestration-carbon-dioxide (accessed on 29 March 2023).

285. Freifeld, B.M.; Daley, T.M.; Hovorka, S.D.; Henninges, J.; Underschultz, J.; Sharma, S. Recent advances in well-based monitoring of CO_2 sequestration. *Energy Procedia* **2009**, *1*, 2277–2284. [CrossRef]

286. Gould, J.; Wackier, J.; Quirein, J.; Watson, J. CO_2 Monitor Logging: East Mallet Unit, Slaughter Field, Hockley County, TX, USA. In Proceedings of the SPWLA 32nd Annual Logging Symposium, Midland, TX, USA, 16–19 June 1991.

287. Müller, N.; Ramakrishnan, T.; Boyd, A.; Sakruai, S. Time-lapse carbon dioxide monitoring with pulsed neutron logging. *Int. J. Greenh. Gas Control* **2007**, *1*, 456–472. [CrossRef]

288. Mito, S.; Xue, Z. Post-Injection monitoring of stored CO_2 at the Nagaoka pilot site: 5 years time-lapse well logging results. *Energy Procedia* **2011**, *4*, 3284–3289. [CrossRef]

289. Xue, Z.; Tanase, D.; Watanabe, J. Estimation of CO_2 Saturation from Time-Lapse CO_2 well Logging in an Onshore Aquifer, Nagaoka, Japan. *Explor. Geophys.* **2006**, *37*, 19–29. [CrossRef]

290. Sakurai, S.; Ramakrishnan, T.S.; Boyd, A.; Mueller, N.; Hovorka, S. Monitoring Saturation Changes for CO_2 Sequestration: Petrophysical Support of the Frio Brine Pilot Experiment. *Petrophysics-SPWLA J. Form. Eval. Reserv. Descr.* **2006**, *47*.

291. Freifeld, B.; Daley, T.; Cook, P.; Trautz, R.; Dodds, K. The Modular Borehole Monitoring Program: A research program to optimize well-based monitoring for geologic carbon sequestration. *Energy Procedia* **2014**, *63*, 3500–3515. [CrossRef]

292. Daley, T.; Miller, D.; Dodds, K.; Cook, P.; Freifeld, B. Field testing of modular borehole monitoring with simultaneous distributed acoustic sensing and geophone vertical seismic profiles at Citronelle, Alabama. *Geophys. Prospect.* **2016**, *64*, 1318–1334. [CrossRef]

293. Liebscher, A.; Möller, F.; Bannach, A.; Köhler, S.; Wiebach, J.; Schmidt-Hattenberger, C.; Weiner, M.; Pretschner, C.; Ebert, K.; Zemke, J. Injection operation and operational pressure–temperature monitoring at the CO_2 storage pilot site Ketzin, Germany—Design, results, recommendations. *Int. J. Greenh. Gas Control* **2013**, *15*, 163–173. [CrossRef]

294. Henninges, J.; Zimmermann, G.; Büttner, G.; Schrötter, J.; Erbas, K.; Huenges, E. Wireline Distributed Temperature Measurements and Permanent Installations Behind Casing. In Proceedings of the World Geothermal Congress, Antalya, Turkey, 24–29 April 2005.

295. Würdemann, H.; Möller, F.; Kühn, M.; Heidug, W.; Christensen, N.P.; Borm, G.; Schilling, F.R. CO_2SINK—From site characterisation and risk assessment to monitoring and verification: One year of operational experience with the field laboratory for CO_2 storage at Ketzin, Germany. *Int. J. Greenh. Gas Control* **2010**, *4*, 938–951. [CrossRef]

296. Sato, K.; Mito, S.; Horie, T.; Ohkuma, H.; Saito, H.; Watanabe, J.; Yoshimura, T. Monitoring and simulation studies for assessing macro- and meso-scale migration of CO_2 sequestered in an onshore aquifer: Experiences from the Nagaoka pilot site, Japan. *Int. J. Greenh. Gas Control* **2011**, *5*, 125–137. [CrossRef]

297. Burgess, K.A.; MacDougall, T.D.; Siegfried, R.W.; Fields, T.G. Wireline-Conveyed Through-Casing Formation Tester Preserves Casing Integrity. In Proceedings of the SPE Eastern Regional Meeting, Canton, OH, USA, 17–19 October 2001.

298. Myers, M.; Stalker, L.; Pejcic, B.; Ross, A. Tracers—Past, present and future applications in CO_2 geosequestration. *Appl. Geochem.* **2013**, *30*, 125–135. [CrossRef]

299. Rein, E.; Schulz, L.K. Applications of natural gas tracers in the detection of reservoir compartmentalisation and production monitoring. *J. Pet. Sci. Eng.* **2007**, *58*, 428–442. [CrossRef]

300. Chandrasekharan, P.; Tay, Z.W.; Zhou, X.Y.; Yu, E.; Orendorff, R.; Hensley, D.; Huynh, Q.; Fung, K.L.B.; VanHook, C.C.; Goodwill, P.; et al. A perspective on a rapid and radiation-free tracer imaging modality, magnetic particle imaging, with promise for clinical translation. *Br. J. Radiol.* **2018**, *91*, 20180326. [CrossRef]

301. Hassoun, S.; McBride, T.; Russell, D.A. Development of perfluorocarbon tracer technology for underground leak location. *J. Environ. Monit.* **2000**, *2*, 432–435. [CrossRef]

302. Dugstad, Ø.; Bjørnstad, T.; Hundere, I.A. Measurements of gas tracer retention under simulated reservoir conditions. *J. Pet. Sci. Eng.* **1993**, *10*, 17–25. [CrossRef]

303. Galdiga, C.U.; Greibrokk, T. Ultra trace detection of perfluorocarbon tracers in reservoir gases by adsorption/thermal desorption in combination with NICI-GC/MS. *Anal. Bioanal. Chem.* **2000**, *367*, 43–50. [CrossRef]

304. Tomich, J.F.; Dalton, R.J.; Deans, H.A.; Shallenberger, L.K. Single-Well Tracer Method To Measure Residual Oil Saturation. *J. Pet. Technol.* **1973**, *25*, 211–218. [CrossRef]

305. Khaledialidusti, R.; Kleppe, J.; Skrettingland, K. Numerical Interpretation of Single Well Chemical Tracer (SWCT) Tests to Determine Residual Oil Saturation in Snorre Reservoir. In Proceedings of the EUROPEC 2015, Madrid, Spain, 1–4 June 2015. [CrossRef]

306. Du, Y.; Guan, L. Interwell Tracer Tests: Lessons Learned from Past Field Studies. In Proceedings of the SPE Asia Pacific Oil and Gas Conference and Exhibition, Jakarta, Indonesia, 5–7 April 2005; p. 9.

307. Stalker, L.; Boreham, C.; Perkins, E. *A Review of Tracers in Monitoring CO_2 Breakthrough: Properties, Uses, Case Studies, and Novel Tracers*; AAPG: Tulsa, OK, USA, 2009; p. 14.

308. Wells, A.W.; Diehl, J.R.; Bromhal, G.; Strazisar, B.R.; Wilson, T.H.; White, C.M. The use of tracers to assess leakage from the sequestration of CO_2 in a depleted oil reservoir, New Mexico, USA. *Appl. Geochem.* **2007**, *22*, 996–1016. [CrossRef]

309. Vandeweijer, V.; van der Meer, B.; Hofstee, C.; Mulders, F.; D'Hoore, D.; Graven, H. Monitoring the CO_2 injection site: K12-B. *Energy Procedia* **2011**, *4*, 5471–5478. [CrossRef]

310. Daley, T.M.; Myer, L.R.; Peterson, J.E.; Majer, E.L.; Hoversten, G.M. Time-lapse crosswell seismic and VSP monitoring of injected CO_2 in a brine aquifer. *Environ. Geol.* **2008**, *54*, 1657–1665. [CrossRef]

311. Lawton, D.; Couëslan, M.; Bland, H.; Jones, M. Seismic Survey Design for Monitoring CO_2 Storage: Integrated Multicomponent Surface and Borehole Seismic Surveys, Penn West Pilot, Alberta, Canada. In Proceedings of the 8th International Conference on Greenhouse Gas Control Technologies, Trondheim, Norway, 19–22 June 2006.

312. Saito, H.; Nobuoka, D.; Azuma, H.; Xue, Z.; Tanase, D. Time-Lapse Crosswell Seismic Tomography for Monitoring Injected CO_2 in an Onshore Aquifer, Nagaoka, Japan. *Explor. Geophys.* **2006**, *37*, 30–36. [CrossRef]

313. Nalonnil, A.; Marion, B. High-Resolution Reservoir Monitoring Using Crosswell Seismic. *SPE Reserv. Eval. Eng.* **2012**, *15*, 25–30. [CrossRef]

314. Zhang, W.; Youn, S.; Doan, Q.T. Understanding Reservoir Architectures and Steam-Chamber Growth at Christina Lake, Alberta, by Using 4D Seismic and Crosswell Seismic Imaging. *SPE Reserv. Eval. Eng.* **2007**, *10*, 446–452. [CrossRef]

315. Sambo, C.; Iferobia, C.C.; Babasafari, A.A.; Rezaei, S.; Akanni, O.A. The Role of Time Lapse(4D) Seismic Technology as Reservoir Monitoring and Surveillance Tool: A Comprehensive Review. *J. Nat. Gas Sci. Eng.* **2020**, *80*, 103312. [CrossRef]

316. Chadwick, R.; Arts, R.; Eiken, O.; Kirby, G.A.; Lindeberg, E.; Zweigel, P. 4D Seismic Imaging of an Injected CO_2 Plume at the Sleipner Field, Central North Sea. *Geol. Soc. Lond. Mem.* **2004**, *29*, 311–320. [CrossRef]

317. Watanabe, S.; Han, J.; Hetz, G.; Datta-Gupta, A.; King, M.J.; Vasco, D.W. Streamline-Based Time-Lapse-Seismic-Data Integration Incorporating Pressure and Saturation Effects. *SPE J.* **2017**, *22*, 1261–1279. [CrossRef]

318. Liang, C.; O'Reilly, O.; Dunham, E.M.; Moos, D. Hydraulic fracture diagnostics from Krauklis-wave resonance and tube-wave reflections. *Geophysics* **2017**, *82*, D171–D186. [CrossRef]

319. Shih, P.-J.R.; Frehner, M. Laboratory Evidence for Krauklis Wave Resonance in Fractures. *Geophysics* **2015**, *81*, T285–T293. [CrossRef]

320. Djuraev, U.; Jufar, S.R.; Vasant, P. A review on conceptual and practical oil and gas reservoir monitoring methods. *J. Pet. Sci. Eng.* **2017**, *152*, 586–601. [CrossRef]

321. Frehner, M. Krauklis Wave Initiation in Fluid-Filled Fractures by a Passing Body Wave. In Proceedings of the Poromechanics V: Proceedings of the Fifth Biot Conference on Poromechanics, Vienna, Austria, 10–12 July 2013; pp. 92–100. [CrossRef]

322. Cao, H. Physical Modeling of the Krauklis Waves: Insights from two Experimental Apparatuses. Diploma Thesis, Michigan Technological University, Houghton, MI, USA, 2020. [CrossRef]

323. Burnison, S.A. *Field Demonstration of CO_2 Injection Monitoring Using Krauklis and Other Guided Waves*; EERC: Grand Forks, ND, USA, 2018.

324. Davis, T.L.; Landrø, M.; Wilson, M. (Eds.) *Geophysics and Geosequestration*; Cambridge University Press: Cambridge, UK, 2019.

325. Carrigan, C.R.; Yang, X.; LaBrecque, D.J.; Larsen, D.; Freeman, D.; Ramirez, A.L.; Daily, W.; Aines, R.; Newmark, R.; Friedmann, J.; et al. Electrical resistance tomographic monitoring of CO_2 movement in deep geologic reservoirs. *Int. J. Greenh. Gas Control* **2013**, *18*, 401–408. [CrossRef]

326. Daily, W.; Ramirez, A.; Labrecque, D.; Nitao, J. Electrical resistivity tomography of vadose water movement. *Water Resour. Res.* **1992**, *28*, 1429–1442. [CrossRef]

327. Karhunen, K.; Seppänen, A.; Lehikoinen, A.; Monteiro, P.J.; Kaipio, J.P. Electrical Resistance Tomography imaging of concrete. *Cem. Concr. Res.* **2010**, *40*, 137–145. [CrossRef]

328. Ramirez, A.; Daily, W.; Labrecque, D.; Owen, E.; Chesnut, D. Monitoring an underground steam injection process using electrical resistance tomography. *Water Resour. Res.* **1993**, *29*, 73–87. [CrossRef]

329. Kiessling, D.; Schmidt-Hattenberger, C.; Schuett, H.; Schilling, F.; Krueger, K.; Schoebel, B.; Danckwardt, E.; Kummerow, J. Geoelectrical methods for monitoring geological CO_2 storage: First results from cross-hole and surface–downhole measurements from the CO_2SINK test site at Ketzin (Germany). *Int. J. Greenh. Gas Control* **2010**, *4*, 816–826. [CrossRef]

330. Schmidt-Hattenberger, C.; Bergmann, P.; Labitzke, T.; Wagner, F.; Rippe, D. Permanent crosshole electrical resistivity tomography (ERT) as an established method for the long-term CO_2 monitoring at the Ketzin pilot site. *Int. J. Greenh. Gas Control* **2016**, *52*, 432–448. [CrossRef]

331. Strickland, C.E.; Vermeul, V.R.; Bonneville, A.; Sullivan, E.C.; Johnson, T.C.; Spane, F.A.; Gilmore, T.J. Geophysical Monitoring Methods Evaluation for the FutureGen 2.0 Project. *Energy Procedia* **2014**, *63*, 4394–4403. [CrossRef]

332. von Hebel, C.; Rudolph, S.; Mester, A.; Huisman, J.A.; Kumbhar, P.; Vereecken, H.; van der Kruk, J. Three-dimensional imaging of subsurface structural patterns using quantitative large-scale multiconfiguration electromagnetic induction data. *Water Resour. Res.* **2014**, *50*, 2732–2748. [CrossRef]

333. Ayani, M.; Grana, D.; Liu, M. Stochastic inversion method of time-lapse controlled source electromagnetic data for CO_2 plume monitoring. *Int. J. Greenh. Gas Control* **2020**, *100*, 103098. [CrossRef]

334. Nabighian, M.N.; Ander, M.E.; Grauch, V.J.S.; Hansen, R.O.; LaFehr, T.R.; Li, Y.; Pearson, W.C.; Peirce, J.W.; Phillips, J.; Ruder, M.E. Historical development of the gravity method in exploration. *Geophysics* **2005**, *70*, 63ND–89ND. [CrossRef]

335. Gasperikova, E.; Hoversten, G.M. Gravity monitoring of CO_2 movement during sequestration: Model studies. *Geophysics* **2008**, *73*, WA105–WA112. [CrossRef]

336. Nooner, S.L.; Eiken, O.; Hermanrud, C.; Sasagawa, G.S.; Stenvold, T.; Zumberge, M.A. Constraints on the in situ density of CO_2 within the Utsira formation from time-lapse seafloor gravity measurements. *Int. J. Greenh. Gas Control* **2007**, *1*, 198–214. [CrossRef]

337. Fabriol, H.; Bitri, A.; Bourgeois, B.; Delatre, M.; Girard, J.; Pajot, G.; Rohmer, J. Geophysical methods for CO_2 plume imaging: Comparison of performances. *Energy Procedia* **2011**, *4*, 3604–3611. [CrossRef]

338. Sugihara, M.; Nawa, K.; Nishi, Y.; Ishido, T.; Soma, N. Continuous Gravity Monitoring for CO_2 Geo-sequestration. *Energy Procedia* **2013**, *37*, 4302–4309. [CrossRef]

339. Power Engineering. Glitter-Sized Sensors That Detect CO_2 Leaks at Storage Sites. 19 December 2022. Available online: https://www.power-eng.com/coal/glitter-sized-sensors-that-detect-co2-leaks-at-storage-sites/ (accessed on 29 March 2023).

340. Sandia National Laboratories. Surveilling Carbon Sequestration: A Smart Collar to Sense Leaks. 13 December 2022. Available online: https://newsreleases.sandia.gov/smart_collar/ (accessed on 29 March 2023).

341. University of Wyoming. SER Researcher Charles Nye Conducts Collaborative Soil Gas Sampling to Advance Wyoming CarbonSAFE Project. 4 September 2021. Available online: http://www.uwyo.edu/ser/news/2021/04/soil-gas-monitoring.html (accessed on 29 March 2023).

342. Gonzalez, K.; Misra, S. Unsupervised learning monitors the carbon-dioxide plume in the subsurface carbon storage reservoir. *Expert Syst. Appl.* **2022**, *201*, 117216. [CrossRef]

343. Ridley, K.; de Villiers, G.; Vovrosh, J.; Vincent, C.; Wilkinson, P.; Holynski, M. Quantum Technology Based Gravity and Gravity Gradiometry as a Tool for CCS Monitoring and Investigation. In Proceedings of the 16th Greenhouse Gas Control Technologies Conference (GHGT-16), Lyon, France, 23–27 October 2022. [CrossRef]

344. White House. *FACT SHEET: President Biden Sets 2030 Greenhouse Gas Pollution Reduction Target Aimed at Creating Good-Paying Union Jobs and Securing U.S. Leadership on Clean Energy Technologies*; U.S. White House: Washington, DC, USA, 2021.